UNIVERSITY OF OKLAHOMA

GRADUATE COLLEGE

EVALUATION OF DURABILITY AND CORROSION BEHAVIOR OF ULTRA-HIGH PERFORMANCE CONCRETE FOR USE IN BRIDGE CONNECTIONS AND REPAIR

A THESIS

SUBMITTED TO THE GRADUATE FACULTY

in partial fulfillment of the requirements for the Degree of

MASTER OF SCIENCE

CIVIL ENGINEERING

By

MARANDA LEGGS
Norman, Oklahoma
2019

Downloaded from SHAREOK. Persistent Handle URL: https://hdl.handle.net/11244/320346

EVALUATION OF DURABILITY AND CORROSION BEHAVIOR OF ULTRA-HIGH PERFORMANCE CONCRETE FOR USE IN BRIDGE CONNECTIONS AND REPAIR

A THESIS APPROVED FOR THE SCHOOL OF CIVIL ENGINEERING AND ENVIRONMENTAL SCIENCE

BY

Dr. Jeffery Volz, Chair

Dr. Royce Floyd

Dr. Gerald Miller

© Copyright by MARANDA LEGGS 2019
All Rights Reserved.

This is dedicated to my loving and supportive grandparents, Brenda and Doug.

Acknowledgements

I would like to first thank everyone that helped me get to this point in my life, so that I could have the opportunity to do this Master's research to begin with. I couldn't have made it this far without the unconditional and overwhelming support from my family, in particular my grandparents Brenda and Doug Hyde. In the same vein, I would also like to give a very special thank you to everyone who helped me get through this research. My devoted research professor Jeffery Volz and his charismatic wife Kathy Volz that made sure I was never bored being her teaching assistant. Royce Floyd, one of, if not the hardest working faculty member in CEES, being both my committee member and the graduate liaison this semester. Gerald Miller, who has come over from the other side of the college, geotechnical engineering, to be here as my other committee member. And of course, a very warm and exhaustive thank you to all of the other research students who helped me get through the day to day in the lab, including Steve, Connor, Raina while she was still here, Jake, and Trevor, who I need to give a special shout out to for all of the many, many heavy things I made him lift for me while I was here. Also, I would like to give a final thank you to my soon to be full-time boss at Jacobs Engineering in Dallas, Tim Potyraj, who has given me a goal (a job) to keep me working towards, and the want to be a successful, and knowledgeable, engineer.

Abstract

Ultra-high performance concrete (UHPC) is one of the new, cutting edge concepts in the world of concrete. Boasting significantly higher compressive and tensile strengths, longer service life, and significantly increased durability, UHPC has a considerable level of appeal over conventional concrete mix designs. This result is accomplished through three main changes to the conventional concrete mix design: an extremely low water-to-cementitious material ratio, elimination of coarse aggregate to allow for dense particle packing, and the addition of steel fibers to significantly increase tensile strength. Unfortunately, these additional advantages come at a significant cost. All commercial UHPC mixtures currently on the market are close to 20 times the price of a traditional concrete mix, pricing most people out of the UHPC market.

The Oklahoma Department of Transportation (ODOT), however, is hopeful and looking for a way to be able to use UHPC for both full and partial bridge deck repairs. Currently, the University of Oklahoma has completed extensive research into developing their own non-proprietary UHPC mix, titled "J3", and found it to be sufficient for all strength and bonding requirements. Still, there is need for research on the durability of J3 before it can be utilized in the field. Quantifying the durability of J3 in comparison to conventional concrete (ODOT class AA), as well as commercially available UHPC (Ductal®), was the primary goal of this study. Testing was broken up into two parts: durability and corrosion. Durability testing included freeze-thaw resistance in accordance with ASTM C666, scaling resistance in accordance with ASTM C672, and chloride ion penetration in accordance with ASTM C1202. Corrosion testing included both small-scale specimen testing to focus solely on the response of each of the different concrete mixtures due to the "Halo Effect", as well as large-scale specimen testing on previously corroded slabs (provided by ODOT) to analyze the overall impact of using different concrete mixtures to repair existing concrete structures with previously corroded steel rebar. Durability results for J3 included a Relative Dynamic Modulus (RDM) value of 103% after 350 freeze-thaw cycles, a visual rating of 0 after 50 scaling cycles, and an average chloride penetration rating of very low and negligible at 28 and 90 days, respectively. Corrosion testing resulted in minimal corrosion of steel reinforcing bars in both the small- and large-scale corrosion specimens. Additionally, significant surface corrosion occurred along the joint of the large-scale Ductal® specimen, which was not experienced by the J3 specimen, proving a superior response to the Halo Effect and overall corrosive attack. The results of this study show J3 to have exceptional durability properties and corrosion resistance, making it ready for trial use as a bridge deck or bridge girder repair material in the field.

Table of Contents

1.0 Introduction 1

1.1 Background and Justification 1

1.2 Project Scope 3

1.3 Objectives and Goals 3

1.3.1 Objectives 4

1.3.2 Goals 4

1.4 Outline 5

2.0 Literature Review 6

2.1 Introduction and Overview 6

2.2 Freeze-Thaw Cycling and Chloride Ion Penetration 8

2.2.1 Basis of Analysis 8

2.2.2 Variable Curing Methods 14

2.2.3 Effects of Silica Powder and Cement Type 20

2.3 Corrosion 24

3.0 Mix Designs and Mixing Procedures 29

3.1 Scope of Work 29

3.2 Mix Designs 30

3.3 Mixing and Curing 33

3.4 Mixture Compressive Strengths 37

4.0 Chloride Ion Penetration, Freeze-Thaw Cycling, and Scaling Resistance Testing 38

4.1 Chloride Ion Penetration 38

4.1.1 Introduction 38
4.1.2 Procedure 39
4.1.3 Testing 41
4.1.4 Summary of Results 43
4.2 Freeze-Thaw Cycling 45
4.2.1 Introduction 45
4.2.2 Procedure 45
4.2.3 Testing 50
4.2.4 Summary of Results 55
4.3 Scaling Resistance 58
4.3.1 Introduction 58
4.3.2 Procedure 58
4.3.3 Testing 60
4.3.4 Summary of Results 65
5.0 Corrosion Testing 67
5.1 Introduction 67
5.2 Small-Scale Corrosion 68
5.2.1 Procedure 68
5.2.2 Testing 71
5.2.3 Summary of Results 77
5.3 Large-Scale Corrosion 78
5.3.1 Procedure 78
5.3.2 Testing 84
5.3.3 Summary of Results 109

6.0 Findings, Conclusions, and Recommendations 110

6.1 Findings.....110

6.1.1 Durability Testing 110

6.1.1 Corrosion Testing.....111

6.2 Conclusions 113

6.3 Recommendations 114

7.0 Appendices.....115

8.0 References.....117

List of Tables

Table 1: Graybeal (2006) Study UHPC Mixture Design 9

Table 2: Scaling Surface Condition Rating System in Accordance with ASTM C672 12

Table 3: Graybeal (2006) Chloride Ion Penetration Results 12

Table 4: Graybeal (2006) Freeze-Thaw Testing Results 13

Table 5: Ahlborn (2011) Study Freeze-Thaw Testing Results 16

Table 6: Chumping (2015) Study Custom UHPC Mix Proportions in kg/m^3 18

Table 7: Chumping (2015) Study Chloride Ion Penetration and Freeze-Thaw Test Results 19

Table 8: Alkaysi (2016) Study Mix Design by Proportion 21

Table 9: Alkaysi Study Chloride Ion Penetration and Freeze-Thaw Test Results 22

Table 10: Chloride Permeability Classifications for Concrete (AASHTO, 1990) 23

Table 11: Hansson (2006) Study Mix Designs in kg/ m^3 27

Table 12: J3 Mix Design 31

Table 13: ODOT Class AA Mix Design 31

Table 14: Ductal® Mix Design 32

Table 15: Concrete Compressive Strengths Summary 37

Table 16: Chloride Ion Permeability Testing Results- 28 Days 43

Table 17: Chloride Ion Permeability Testing Results- 90 Days 43

Table 18: Chloride Permeability Classifications for Concrete 44

Table 19: Freeze-Thaw Testing Results 56

Table 20: Scaling Surface Condition Rating System in Accordance with ASTM C672 59

Table 21: Average Scaling Visual Rating Results 65

Table 22: Measured Voltage (V) at Conclusion of Initial Testing Between Adjacent Steel Reinforcing Bars in 0% NaCl Small-Scale Corrosion Specimens 115

Table 23: Graybeal (2018) Study Mix Design in lb/yd^3 115

Table 24: Graybeal (2018) Study Results 115

List of Figures

Figure 1: Graybeal (2006) Chloride Ion Specimen Post-Testing 13

Figure 2: 0.5 in. Steel Fibers.....32

Figure 3: J3 before "Break Over" 34

Figure 4: J3 after "Break Over" 35

Figure 5: First Half of Small-Scale Corrosion Specimens 36

Figure 6: AA Large-Scale Corrosion Specimen (left) and Durability Specimens (right).....36

Figure 7: Ductal® Large-Scale Corrosion Specimen (left) and Durability Specimens (right) 36

Figure 8: J3 Durability Specimens (left) and Phoscrete Durability Specimens (right) 37

Figure 9: Vacuum Pump (right) and Desiccator (left) 40

Figure 10: Chloride Ion Permeability Testing Using PROOVE'it- Typical 41

Figure 11: State of Chloride Ion Penetration Testing Specimens After 28 Day Testing for 42

Figure 12: Freeze-Thaw Specimen in Testing Machine 48

Figure 13: Typical Emodumeter Transverse Frequency Measurement 48

Figure 14: Typical Emodumeter Transverse Frequency Output Page.....49

Figure 15: Freeze-Thaw Specimens in the Testing Chamber- Cycle 0 50

Figure 16: Condition of All Freeze-Thaw Specimens- Cycle 0 51

Figure 17: Deteriorated State of an AA Freeze-Thaw Specimen- Cycle 350 51

Figure 18: Deteriorated State of a Ductal® Freeze-Thaw Specimen- Cycle 350 52

Figure 19: Deteriorated State of a J3 Freeze-Thaw Specimen- Cycle 350 53

Figure 20: Hole Formed on the Side of Ductal® Freeze-Thaw Specimen- Cycle 315 53

Figure 21: Surface Corrosion of Ductal® Freeze-Thaw Specimen- Cycle 350.....55

Figure 22: Average RDM Values Over 350 Cycles of Freeze-Thaw Testing 56

Figure 23: Condition of Scaling Specimens- Cycle 0 60
Figure 24: Visual Pocketing on AA Specimen- 25 Cycles 61
Figure 25: Visual Corrosion of Steel Fibers on Ductal® Specimen- 25 Cycles 61
Figure 26: Visual Examination of Scaling Specimen at 50 Days for (a) ODOT AA 63
Figure 27: Progression of Visual Pocketing on AA Specimen- 50 Cycles 64
Figure 28: Visual Pocketing on Ductal® Specimen- 50 Cycles 64
Figure 29: Small-Scale Corrosion Specimen Molds 70
Figure 30: Typical Small-Scale Corrosion Testing Set-Up 70
Figure 31: Joint Corrosion in Ductal® Small-Scale Corrosion Testing Specimen- Patching 72
Figure 32: Joint Corrosion in Ductal® Small-Scale Corrosion Testing Specimen- Corrosion Spotting 72
Figure 33: Steel Rebar Before Testing- Typical 74
Figure 34: Corrosion State of Rebar Reinforcing at Joint of AA Small-Scale Corrosion Specimens with (a) 4% NaCl (b) 8% NaCl 75
Figure 35: Corrosion State of Rebar Reinforcing at Joint of J3 Small-Scale Corrosion Specimens with (a) 4% NaCl (b) 8% NaCl 76
Figure 36: Corrosion State of Rebar Reinforcing at Joint of Ductal® Small-Scale Corrosion Specimens with (a) 4% NaCl (b) 8% NaCl 76
Figure 37: Corrosion State of Rebar Reinforcing at Joint of Phoscrete Small-Scale Corrosion Specimens with (a) 4% NaCl (b) 8% NaCl 77
Figure 38: Joint Specimens before Chipping 79
Figure 39: Joint Specimens after Chipping 80
Figure 40: Joint Specimen Rebar Fully Tied Together 80
Figure 41: Stainless Steel Rod and Electrical Wiring for Large-Scale Corrosion Testing 82

Figure 42: Large-Scale Corrosion Testing Set-up 83
Figure 43: White Film in Water of Large-Scale Corrosion Specimen- Phoscrete 85
Figure 44: Corrosion in Water of Large-Scale Corrosion Specimens- Typical 85
Figure 45: Joint Corrosion in Ductal® Large-Scale Corrosion Testing Specimen- Week Two (Ductal® on left side of image) 86
Figure 46: Joint Corrosion in Ductal® Large-Scale Corrosion Specimen- Week Five.....87
Figure 47: Green Liquid in Joint of Phoscrete Large-Scale Corrosion Specimen- Week 7 88
Figure 48: Green Liquid in Joint of Ductal® Large-Scale Corrosion Specimen- Week 8 89
Figure 49: Green Liquid in Joint of Phoscrete Large-Scale Corrosion Specimen- Week 10.....90
Figure 50: Green Liquid in Joint of Ductal® Large-Scale Corrosion Specimen- Week 10 90
Figure 51: Visible Confirmation of Corrosion of Vertical Reinforcing Bars- Week 1 92
Figure 52: Typical Level of Corrosion at the Conclusion of Testing- Week 10 92
Figure 53: Chipping Sequence of Large-Scale Corrosion Specimens 93
Figure 54: Week 1 Update of Large-Scale Corrosion Specimens Using (a) ODOT AA (b) J3 (c) Ductal® (d) Phoscrete.....94
Figure 55: Week 3 Update of Large-Scale Corrosion Specimens Using (a) ODOT AA (b) J3 (c) Ductal® (d) Phoscrete.....95
Figure 56: Week 6 Update of Large-Scale Corrosion Specimens Using (a) ODOT AA (b) J3 (c) Ductal® (d) Phoscrete.....96
Figure 57: Week 10 Update of Large-Scale Corrosion Specimens Using (a) ODOT AA (b) J3 (c) Ductal® (d) Phoscrete.....97
Figure 58: First Chip of Large-Scale Corrosion Specimens Using (a) ODOT AA (b) J3 (c) Ductal® (d) Phoscrete.....98

Figure 59: Second Chip of Large-Scale Corrosion Specimens Using (a) ODOT AA (b) J3 (c) Ductal® (d) Phoscrete....99
Figure 60: Fourth Chip of Large-Scale Corrosion Specimens Using (a) ODOT AA (b) J3 (c) Ductal® (d) Phoscrete....100
Figure 61: Fifth Chip of Large-Scale Corrosion Specimens Using (a) ODOT AA (b) J3 (c) Ductal® (d) Phoscrete....101
Figure 62: Fifth Chip of Large-Scale Corrosion Specimens 24 Hours After Chipping Using (a) ODOT AA (b) J3 (c) Ductal® (d) Phoscrete....102
Figure 63: Evidence of Surficial Corrosion on Large-Scale Corrosion Specimens Using (a) J3 (b) Ductal® (c) Phoscrete....106
Figure 64: Graph of the Change in Voltage over Time of all Large-Scale Corrosion Specimens....107
Figure 65: Final State of Phoscrete Large-Scale Corrosion Specimen- Week 10....108
Figure 66: Numbering for Measurements of Voltage Between Adjacent Steel Reinforcing Bars....116

1.0 Introduction

This chapter will introduce the motivation for testing and classification of durability and corrosion properties of a non-proprietary ultra-high-performance concrete (UHPC) developed by the University of Oklahoma using locally sourced materials. Additionally, this section includes a discussion of the scope, objectives, and goals of this research study, as well as providing an outline of this thesis.

1.1 Background and Justification

In the 1990s, Reactive Powder Concrete (RPC) began to be developed to combat two major issues of conventional concrete: low tensile capacity and a lack of durability. This was done by removing course aggregate to improve the concrete homogeneity, and therefore the concrete properties through dense particle packing (Jones, 1996). From there, UHPC was developed with the addition of fiber reinforcing for extra tensile strength. The most widespread and well researched UHPC on the market today is a product called Ductal®, by Lafarge. Ductal® has some of the most impressive strength and durability properties of researched UHPC, including a compressive strength in excess of 30 ksi. However, this strength comes with a hefty price tag, in upwards of $3,000 per cubic yard (for comparison, conventional concrete typically costs approximately $150 per cubic yard). Ductal's® availability means that it is utilized in almost all current UHPC construction; however, its large price tag means that most projects simply do not get the option to use UHPC at all.

This high cost of commercial UHPC is the reason for the significant amount of research across the country, in large part by the Federal Highway Administration (FHWA), to develop more cost-effective mix designs with locally sourced materials. According to FHWA, UHPC should have a minimum compressive strength of 21.7 ksi, a water-to-cementitious material (w/cm) ratio equal to or less than 0.25, and a post-cracking tensile strength of at least 0.72 ksi (Graybeal 2011), a definition that will be used throughout this study.

It is the intent of the Oklahoma Department of Transportation (ODOT) to continue research into a cost-effective UHPC mix from materials available in Oklahoma that completely fulfills the description specified by FHWA. Specifically, ODOT is interested in the use of UHPC for bridge connections and repairs, since the utilization of UHPC can result in significantly increased life spans for bridges, while decreasing the number of repairs needed over this extended useable life.

For Phase I of this research, titled simply "Evaluation of Ultra-High Performance Concrete for Use in Bridge Connections and Repair", an initial non-proprietary mix design, using local materials and meeting all FHWA's basic requirements, was developed. This design was meant to be used in all subsequent testing for an even foundation of analysis, with modifications made based on all data gathered from following Phase I and Phase II testing to develop an optimum mix design for all UHPC potential applications.

To develop this mix design, an original 3,400 potential mix designs were considered, based on computer analyses for optimal particle packing. From there, nine series of mix design trail batches were conducted using various types of cement, supplementary cementitious materials

(SCM), admixture quantities, sand types, and w/cm ratios. The ultimate mix design chosen is titled “J3”. This mix design was chosen as the best alternative because of its workability when mixed with steel reinforcing fibers, high early compressive strength, and expected durability. Table 12 in Section 3.2 details the exact mix for J3 to be used throughout this study (McDaniel 2017).

1.2 Project Scope

During Phase I testing of a full scale joint replacement on a SH-3E bridge over the N. Canadian River in Oklahoma, a concern was raised as to whether the use of UHPC as a repair material would “simply push existing corrosion activity into the existing bridge deck or accelerate corrosion in the area surrounding the joint” (Floyd and Volz, 2018). This concern, as well as the need to classify the durability properties of J3, is the primary basis for this study, which focuses on two major parts of Phase II testing: corrosion and durability. Durability testing included chloride ion penetration, freeze-thaw cycling, and scaling resistance, while corrosion testing was performed on both small- and large-scale specimens.

1.3 Objectives and Goals

As mentioned, this study is a single part of a larger multi-phase project for the Oklahoma Department of Transportation (ODOT) (Floyd et al., 2016). The overall end goals of this project include: identifying available and appropriate locally sourced UHPC materials to make a UHPC mix design to be used for bridge repair, evaluating best practices and performance of trial joints,

and creating specifications regarding UHPC use in the state of Oklahoma. The following are the specific objectives and goals for the part of the project covered in this thesis.

1.3.1 Objectives

The objectives for this study include the following:

1. Determine the effect of using UHPC in bridge joints with existing corrosion.
2. Quantify the durability properties of the University of Oklahoma local UHPC alternative J3.
3. Assess the usability of the University of Oklahoma local alternative J3 over proprietary products based on durability.
4. Make recommendations to ODOT as to whether J3 should be used in future ODOT projects.

1.3.2 Goals

The goals for this study include the following:

1. To verify that the non-proprietary UHPC mix design J3 is suitable for field use based on durability criteria.
2. Confirmation that J3 does not increase corrosion in existing structures when used as a bridge repair material, as compared to other commonly used repair materials.

1.4 Outline

This thesis consists of six chapters. Chapter 1 provides a brief background and justification for the study, as well as an outline of the scope, objectives, and goals of the research. Chapter 2 summarizes the literature relevant to the study, including the topics of freeze-thaw cycling, scaling resistance, chloride ion penetration, and corrosion.

Chapter 3 outlines the mix design and mixing procedure used to construct all of the testing specimens used throughout this study. Chapter 4 addresses the durability testing, including the procedure, testing, and a summary of results for the chloride ion penetration, freeze-thaw, and scaling resistance testing. Chapter 5 addresses the corrosion testing, including the procedure, testing, and a summary of results for both the small- and large-scale testing. Chapter 6 summarizes the findings, conclusions, and recommendations of this research study.

2.0 Literature Review

2.1 Introduction and Overview

"Overall, the greatest impact of UHPC materials may lie in the improved durability of concrete structures, [which] leads to lower bridge repair costs and less downtime for repair. The need for a structural material to perform in harsh environments is a reality, whether the structure is a local bridge subjected to constant winter salting or a bridge pier enduring the harsh freezing and thawing of the Straits of Mackinac." –Characterization of Strength and Durability of Ultra-High Performance Concrete under Variable Curing Conditions (Ahlborn 2011)

There is no denying UHPC's superiority when it comes to compression and tensile strength. However, its greatest strength might actually come from its extreme durability. With its discontinuous pore structure, low w/c ratios, and dense particle packing, liquid ingress becomes virtually impossible, greatly reducing huge factors of potential risk on exposed concrete like freeze-thaw (since UHPC has no residual water and there is no room for water to get in) and chloride ion penetration.

It makes sense then that intensive projects, or projects in high risk areas, would choose to use UHPC not just for its exceptional strength, but specifically for its durability. Toutlemonde and Resplendino (2011) describe multiple such projects. One exceptional case being two girders poured in 1996 made out of RPC, made to support an air cooling tower in the Cattenom nuclear power plant in eastern France. After 10 years in service, constantly surrounded by furring water with a chloride content between 1.0 and 2.0 g/l, core sampling of the girders revealed that not

only had the concrete stopped all corrosion of completely encased fibers and steel reinforcing, but ultimately had a chloride ion level of less than 0.10 g per 100 g of cement (where 0.40 g per 100 g is typically the limit for a highly corrosive environment).

Another similar case discussed by Toutlemonde and Resplendino (2011) is a weir at Eraring power station in New South Wales, Australia, along Lake Macquarie. This weir was protected by a spray cover made of precast, pre-tensioned concrete panels, to guard against the constant ocean salt water spray coming off nearby rocks. Using conventional concrete, these precast panels lasted a mere 14 years before they began to collapse from corrosion. UHPC replacement panels were chosen because they could then be significantly thinner, and therefore lighter, and are expected to have a lifespan of at least 100 years, if not "five times that" (pp. 199).

Although the U.S. has not used UHPC on large projects for quite as long as other places in the world, there are projects in the U.S. that utilize UHPC for similar purposes, such as the Pulaski Skyway in New Jersey, which did a partial fill to help the bridge continue to stay in use throughout a larger reconstruction effort, despite its heavy wear and special need of high weather resistance (Mcdonagh and Foden, 2016). ODOT wishes to follow suit in using UHPC in situations where corrosion or durability failure could be quite catastrophic, like bridge joint repairs.

However, these durability properties need to be properly quantified to be able to evaluate the University of Oklahoma non-proprietary mix in regards to acceptable limits of deterioration in both appearance and strength. Following is a discussion of five previous studies over varying

durability topics to establish an understanding of exactly how a UHPC mix should perform with regards to durability testing. The mix used in each study, if it is a non-standard UHPC mix design, will be described in detail, since any change in design such as curing regimen or material gradation can have a large impact on the strength and additional resilience properties of the mix. Also specially noted is the mixing procedure for each study, since they vary widely to achieve the high-shear mixing regimen necessary for UHPC.

2.2 Freeze-Thaw Cycling and Chloride Ion Penetration

2.2.1 Basis of Analysis

There is currently a reasonably large amount of work from around the world focused on UHPC, with much of the work done in the U.S. coming from one source specifically: Benjamin Graybeal and the Federal Highway Administration (FHWA). The largest of these pieces of work by far is the 2006 Graybeal study "Material Property Characterization of Ultra-High Performance Concrete", which made an effort to test a standard Ductal® mix (detailed in Table 1) for every type of behavior, including strength-based, long-term stability, and durability. In 2007, an article was written for the Journal of Materials in Civil Engineering by Benjamin Graybeal and Jussara Tanesi that acted as an abstract of the 2006 study by taking out and discussing only the durability testing performed during the 2006 study. The results presented in this 2007 article will be discussed here as a basis of understanding for UHPC durability properties.

Table 1: Graybeal (2006) Study UHPC Mixture Design

Material	Amount (kg/m^3)	Percent by weight
Portland Cement	712	28.5
Fine Sand	1,020	40.8
Silica Fume	231	9.3
Ground Quartz	211	8.4
Superplasticizer	30.7	1.2
Accelerator	30.0	1.2
Steel Fibers	156	6.2
Water	109	4.4

Throughout this study, four curing regimes were tested: ambient air, 48-hour standard steam treatment (90°C and 95% Relative Humidity) applied immediately, 48-hour standard steam treatment applied 15 days after casting, and 48-hour tempered steam treatment (60°C and 95% Relative Humidity) applied immediately. The mixing regime was not specified beyond the fact that each 0.03 m^3 batch took approximately 20 minutes of final mixing to allow for complete fiber dispersal.

Chloride ion penetration testing was performed using ASTM C1202 standards. For each curing regime, three specimens (51 mm thick x 102 mm in diameter) were tested for their ability to resist chloride penetration by measuring the amount of electrical current that passed through them over a 6-hour period using a 60 V direct current. During testing a 3% NaCl solution was applied to one side of each specimen while a 0.3 N NaOH solution was applied to the other side. Chloride ion penetration testing was also performed according to the AASHTO T259-80

specification, but all results were found to be below the minimum accuracy threshold for the testing method, indicating extremely low values of chlorides present in all cases (Graybeal, 2006).

Freeze-thaw testing was performed in accordance with ASTM C666 Procedure A on three prisms for each curing regime, each 76 mm x 102 mm x 406 mm in size, by varying the freezing and thawing environment from -18°C to 4.4°C for over 690 cycles. This aggressive environment testing helps to determine the microstructure of the concrete and how well it can combat water ingress and expansion due to freezing. The resonant frequencies of each specimen were measured periodically to gauge these microstructures, as well as to calculate the relative dynamic modulus' (RDM) of each specimen, which was calculated by dividing each measured resonant frequencies by the original frequency measured priori to testing. RDM is the typical measurement in ASTM C666 to determine the deterioration of the concrete, with 100% being the starting RDM for each specimen. RDM values between 95% and 100% were found for all of the curing regimes, except for ambient air, which got to RDM values exceeding 110% (Graybeal, 2006). The unusually high values for the ambient air/untreated specimens lead to further testing in which specimens of the four curing regimes were placed just in air or water for 28 days before their RDM's were measured. These tests concluded that due to greater proportions of unhydrated cementitious particles (which could be hydrated and therefore swell) untreated UHPC has an increased permeability that can allow ingress of greater amounts of water that can show up as an extremely large RDM value before it shows up as deterioration, even in harsh Freeze-Thaw conditions. Visible pitting on untreated/ambient air specimens during Freeze-Thaw testing does

indicate, however, that untreated specimens could perhaps have more long-term deterioration that does not show up when only measuring RDM values (Graybeal, 2006).

Scaling resistance, which measures concrete performance under winter conditions of high levels of freeze-thaw while also applying deicing chemicals, was measured using ASTM C672. This test is not performed by many other studies because freeze-thaw testing is typically thought to be sufficient, but it is planned for in this research study for a more complete analysis, so it will be discussed here.

In this Graybeal study, scaling resistance testing involved the testing of two slabs, each 356 mm x 356 mm x 76 mm deep, for each curing regime. Initially, the test was to be performed by ponding a solution of CaCl on the side of each slab that was cast downward, placing them in an environment that went from -18°C for 18-hours to 23°C for 6-hours, and letting them run for at least 50 cycles. Unfortunately, the lower temperature could not be reached for the first 50 cycles using a walk-in freezer, so an additional 145 cycles were performed under the prescribed values using an environmental chamber. After all of the cycles were completed, the slabs were drained and visually inspected. Less than 0.5 g of various material was collected from the surface of each slab, and there was no visual difference between any of the eight slabs, all having no surface scaling. Overall, a surface condition rating of 0 was given to all eight slabs in accordance with ASTM C672, as described in Table 2 (Graybeal, 2006).

Table 2: Scaling Surface Condition Rating System in Accordance with ASTM C672

Rating	Condition
0	No scaling
1	Very slight scaling (3 mm [1⁄8 in.] depth, max, no coarse aggregate visible)
2	Slight to moderate scaling
3	Moderate scaling (some coarse aggregate visible)
4	Moderate to severe scaling
5	Severe scaling (coarse aggregate visible over entire surface)

Results from chloride ion penetration and freeze-thaw tests are given in Tables 3 and 4. A specimen at the end of the Graybeal (2006, 2007) chloride ion penetration testing is shown in Figure 1.

Table 3: Graybeal (2006) Chloride Ion Penetration Results

Curing Regime	Age	Average Coulombs Passed
Steam	28	18
Ambient Air	28	360
Ambient Air	56	76
Tempered Steam	28	39
Tempered Steam	56	26
Delayed Steam	28	18

Table 4: Graybeal (2006) Freeze-Thaw Testing Results

Curing Regime	RDM after 300 cycles (%)	RDM After 690 Cycles (%)
Ambient Air	110	112
Standard Steam	97	96
Delayed Steam	99	98
Tempered Steam	100	100



Figure 1: Graybeal (2006) Chloride Ion Specimen Post-Testing

All results from Graybeal (2006) testing showed what was expected: high durability properties for UHPC. Specifically, all specimens were found to have near perfect or even exceptionally high RDM values, even after undergoing twice the necessary number of freeze-thaw cycles, as well as chloride ion levels in the negligible range (excluding ambient air specimens at 28 days, which were still in the low range). The only unexpected part of the study is the significant drop of chloride ingress between the 28 day and 56 day ambient air specimens only, which is likely due to the fact that the extremely high amounts of cementitious material in UHPC (which are

necessary to develop its dense particle packing) often take more than 28 days to fully cure. This is especially true of silica fume, of which there was a significant amount in the Ductal® mix used.

Similar to the 2006-2007 study, a study was performed in 2018 by Graybeal in conjunction with the FHWA to examine six different commercially available UHPC-class materials. Durability testing was done for five out of the six mixtures through both freeze-thaw cycling and chloride ion penetration testing. Descriptions of the five mix designs tested for durability and their corresponding durability results are presented in the Appendix as Tables 23 and 24, respectively.

2.2.2 Variable Curing Methods

However, Graybeal's work alone is not enough to go on. Many studies have come out since Graybeal's original UHPC studies in 2006-2007 expanding on what he found and giving comparison to his results. Certainly needed is an analysis that uses other ways to measure freeze-thaw resistance to evaluate the accuracy of RDM analysis. For this, there is the 2011 study by Theresa Ahlborn for the Michigan Technology University, "Characterization of Strength and Durability of Ultra-High Performance Concrete under Variable Curing Conditions". In this study, a standard Ductal® UHPC mix was tested using both freeze-thaw cycling and chloride ion penetration, with a focus throughout the study also put on the different curing regimes used. These curing methods included: ambient air, 48-hour thermal steam treatment applied immediately and 48-hour thermal steam treatment applied at a 10 and 24 day delay before curing. Care was used in this study to follow the Ductal® procedure for high shear mixing and

steam curing, as well as to follow ASTM and AASHTO methods for testing as closely as possible, except where doing so might interfere with curing regimens. The only change this led to in our areas of concern was that before freeze-thaw cycling, the specimens were not soaked in a lime bath for 48 hours like ASTM C666 outlines, but due to the impermeability of UHPC, it is not likely that these specimens would have gotten to full saturation anyway, so it is unlikely that this change had any effect on the outcome of the freeze-thaw tests.

For this study, chloride ion penetration testing and preparation followed ASTM C1202 exactly for adequate comparison to other concrete types. The curing regimes tested were 28 day ambient air-cured, 7 day thermal steam treated (applied immediately), and 28 day thermal steam treated (applied immediately), with four specimens 2 in. thick x 4 in. in diameter (51 mm x 102 mm) being cast for each curing treatment. All specimens were tested 28 days after initial pour for equivalent comparison. The specimens were cast 3 in. high and cut from the top one day before treatment, with the bottom surface representing the bridge or deck element surface and being exposed to the 3% NaCl during testing (with the other side being exposed to the 0.3 N NaOH). The results of this analysis showed that no matter the curing regime, the total charge passing through the specimens was negligible (<100 coulombs), with the air cured specimens experiencing a slightly higher average total charge, 75 C, versus the thermal steam treated specimens, which experienced a 10 C average for the 7-day specimens and 15 C for the 28-day specimens. It is noted in this study that “the ionic movement was independent of whether the [thermal steam] treated specimens [were] tested at 7 or 28 days within a 95% confidence interval” (Ahlborn, 2011), a statement that heavily supports the results collected by Graybeal (2007). Unfortunately, the large drop over time of chloride penetration of ambient air specimens

could not be confirmed in this study because ambient air specimens were only tested at one age, 28 days.

There was a slight concern during this study of short circuiting the testing machine during chloride ion penetration testing due to the inclusion of steel fibers in the UHPC. This did not occur during this study, but a note of this concern was carried forward into testing.

Freeze-thaw (Freeze-Thaw) cycle testing was performed on four 3 in. x 4 in. x 16 in. (75 mm x 100 mm x 406 mm) beams for both ambient air and thermal steam treated (applied immediately) curing methods. All specimens were subjected to eight freezing in air and thawing in water cycles per day for at least 300 cycles in accordance with ASTM C666 Procedure B. Relative dynamic modulus (RDM), length change, and mass change were measured for these specimens approximately every 32 cycles, giving a wide range of properties for analysis of Freeze-Thaw resistance. Additionally, three ambient air cured and three thermal steam treated specimens were cycled in and out of a separate, ambient temperature, water bath for comparison. These wet-dry (W-T) specimens were only measured for mass change and RDM values. The results for all 14 specimens are shown in Table 5.

Table 5: Ahlborn (2011) Study Freeze-Thaw Testing Results

Curing and Testing Regime	No. of Specimens	Average RDM at End of Cycling (%)	Average Length Change (%)	Average Mass Change (%)
Air (F-T)	4	101.57	0.0004	0.54
TT (F-T)	4	100.27	0.000014	0.08
Air (W-D)	3	101.91	—	0.22
TT (W-D)	3	100.10	—	0.06

According to ASTM C666, a specimen has considered to have failed due to freeze-thaw when its RDM reaches 60% of its initial modulus, or if the specimen has expanded 0.10% in length. As seen in Table 5, none of the specimens tested in this study came anywhere near these failure criteria, with all specimens actually finishing with a RDM higher than 100% (meaning that instead of deteriorating, these specimens simply continued to hydrate). It can also be seen that air cured specimens had overall significantly higher increases compared to the thermal steam treated specimens, primarily due to the fact that the air cured specimens have more un-hydrated cement particles that become hydrated in the presence of water, even under the harsh conditions of freeze-thaw cycling, just as was experienced in the 2007 Graybeal study, though to a significantly lesser extent. Also important to note is that the found length and mass changes were seen to be in good correlation to the RDM values, so RDM values are all that will be presented for this thesis research.

Another similar study was conducted in 2015, funded by the National Natural Science Foundation of China, to investigate the effects of different curing conditions on UHPC durability properties while also experiencing a flexural load (Chumping et al.). In this study, three different curing conditions were studied: standard ambient air curing, thermal steam curing, and oven curing. A special loading device was used on all loaded specimens in this study to make the specimens act as four-point bending beams under 50% ultimate flexural load. All specimens tested were 40 mm x 40 mm x 160 mm with fine steel fibers 0.2 mm in diameter x 13 mm in length. The mixing procedure for this study was not detailed, but the custom UHPC mix used is presented in Table 6. This study hoped to assess UHPC for effectiveness in areas with harsh durability conditions and high loading/intense use requirements in parallel.

Table 6: Chumping (2015) Study Custom UHPC Mix Proportions in kg/m^3

Cement	Fly Ash	Silica Fume	River Sand	Superplasticizer	Water	Steel Fiber
540	432	108	1,296	37.8	172.8	160

Chloride diffusion testing was performed by painting the specimens with epoxy on all sides except for one exposed side to be tested, which was placed in the tensile region. The specimens were then immersed in a sealed container of 10% by weight sodium chloride for 90 days, after which powder samples were collected by drilling holes at different depths in the exposed surface and free chloride contents were found using titration methods. Freeze-thaw testing was performed in accordance with Chinese standard GB/T 50082-2009, which involved alternating the specimens between -20°C and 20°C in a freeze-thaw box, with one cycle taking about 4 hours. Every 50-100 cycles, the specimens were taken out and measured for RDM and mass loss, with over 800 total cycles performed for each specimen. For both tests, loaded and non-loaded specimens were examined for comparison, with all loaded specimens simply being put into their testing conditions while also being in the loading apparatus mentioned above.

Table 7: Chumping (2015) Study Chloride Ion Penetration and Freeze-Thaw Test Results

Curing Method	Avg. Cl Penetration at <5 mm depth-Non-Loaded (%)	Avg. Cl Penetration at <5 mm depth-Loaded (%)	Avg. Cl Penetration at 5-10 mm depth-Loaded (%)	Mass Loss After 800 F-T Cycles-Loaded (%)	RDM After 800 F-T Cycles-Loaded (%)
Standard	0.125	0.15	<0.05	1.10	95.30
Steam	0.13	0.15	<0.05	1.16	94.35
Oven	0.225	.275	0.125	1.35	92.62

A summary of key test results from this study is presented in Table 7. An important testing result not reflected in Table 7 was that for all specimens, regardless of curing type or whether they were loaded or non-loaded, mass loss was similar before 300 cycles, an indication that perhaps the Ahlborn study could have benefited from performing more cycles in their Freeze-Thaw testing. After 300 cycles, the loaded specimens began to exhibit more mass loss than the non-loaded ones. It should also be noted that mass loss stayed around 0.50% maximum for all curing methods without loading applied and even the worst case of oven cured specimens only got down to about 95% RDM without loading applied.

These results show conclusively no failure of this UHPC mix, with all average chloride ion penetration levels well below the limit for a highly corrosive environment mentioned before of 0.40% and RDM's well above the 60% ASTM C666 limit. These results also indicate that oven curing leaves the UHPC much more vulnerable to chloride ion penetration and Freeze-Thaw losses. This is due to the fact that oven curing causes concrete to actively lose water, leaving it with micro-cracks. Micro-cracks not only lead to paths for chloride ions to enter, but also induce

spalling of the specimen surfaces in Freeze-Thaw testing, which is the main cause of mass loss. However, perhaps the most surprising result from this study is that while loading the specimens does of course result in a predictable decrease in durability properties, this decrease is no more dramatic than that from any other change, like curing regime. Moreover, even with loading applied and poor curing conditions (in regards to durability properties) all specimens are well within working conditions. This truly goes to illustrate just how much any change when working with UHPC can result in a large difference in durability results. Yet, no matter how many changes are made, even when in conjunction to one another, UHPC continues to impress with its durability properties.

2.2.3 Effects of Silica Powder and Cement Type

Ahlborn (2011) mentions in her study that for materials that contain high amounts of silica fume and silica powder, like UHPC, it is very common to have a lower chloride ion movement rate than that normally found in materials without silica fume. However, no research had been done at the time to officially make this correlation for UHPC specifically. Since J3 includes the use of a significant amount of silica fume but no silica powder, this hypothesis needed to be looked into further.

In 2016, a study by Alkaysi et al. at the University of Michigan was done using nine different UHPC mixes to try to get a better understanding of the effects that different cements and amounts of silica powder can have on UHPC. Mix proportions and designations for these nine mixes are summarized in Table 8. Three different cement types were used: a Type I white

cement, a Type V Portland cement, and a 50:50 blend of Type I Portland cement and GGBFS (ground granulated blast-furnace slag). All mixes incorporate two types of silica sand, F100 and F12, which have a median particle size of 100 and 500 μm, respectively. All of the mix designs used steel fibers that were 19 mm long with a diameter of 0.2 mm and were mixed with a horizontal pan mixer using standard dry mixing procedures, like those to be used in this thesis research.

Table 8: Alkaysi (2016) Study Mix Design by Proportion

Name	White Cement	Silica Fume	Silica Powder	Fiber (%)	F100	F12
W-25	1.0	0.25	0.25	1.50	0.26	1.06
W-15	1.0	0.25	0.15	1.50	0.29	1.14
W-00	1.0	0.25	0.00	1.50	0.31	1.26
	Portland Type V					
V-25	1.0	0.25	0.25	1.50	0.26	1.05
V-15	1.0	0.25	0.15	1.50	0.28	1.14
V-00	1.0	0.25	0.00	1.50	0.31	1.26
	Type I/GGGBS Cement					
IG-25	1.0	0.25	0.25	1.50	0.26	1.06
IG-15	1.0	0.25	0.15	1.50	0.28	1.14
IG-00	1.0	0.25	0.00	1.50	0.31	1.26

In this study, two cylindrical specimens, 150 mm in diameter and 300 mm in height, for each of the nine concrete mixes were cast for freeze-thaw testing. After 24 hours of curing, the cylinders were demolded and submerged in ambient temperature water for 28 days before being cut into 120 mm x 110 mm x 70 mm rectangular prisms. From there, the lateral surfaces of the prisms were sealed with aluminum foil using butyl rubber and each prism was placed with their bottom

horizontal surface in the testing liquid. Each cycle was done over a 12-hour period by varying the temperatures of the Freeze-Thaw system from -20°C to 20°C. This study used a modified CIF (capillary suction, internal damage, and freeze-thaw) testing procedure to properly measure the resistance of each concrete mix to combined attack from de-icing salt and frost, similar to scaling resistance testing. Moisture uptake and internal damage were measured every few cycles for at least 60 cycles (a relatively low number of cycles, though understandable for the number of mix designs tested). After 28 cycles, total mass losses (presented in Table 9) were compared to the limit for mean scaling of 1500 g/m^2 and found to be significantly lower for all nine mixes. After 60 cycles, it was also concluded that none of the nine mixes had RDM's lower than 100% (i.e., no internal damage).

Table 9: Alkaysi Study Chloride Ion Penetration and Freeze-Thaw Test Results

UHPC Mix	Total Charge Passed- Rapid Chloride Ion Penetration (Coulombs)	Total Mass Loss after 28 cycles (g/m^2)- F-T
W-25	89	98.8
W-15	295	20.7
W-00	637	17.7
V-25	939.5	18.2
V-15	488.5	18.0
V-00	57	42.2
IG-25	137.5	20.5
IG-15	229	24.2
IG-00	137.5	44.7

In accordance with ASTM C1202, chloride penetration testing was done on 100 mm diameter x 500 mm width specimens, two for each of the nine mix designs, using a measurement cell with a fluid reservoir on both horizontal face of each specimen. One reservoir was filled with a 3% NaCl solution connected to a negatively charged terminal and the other with a 0.3 N NaOH

solution connected to a positively charged terminal. Electrical current was then automatically measured for a standard 6-hour period with a direct current voltage of 60 V. When compared to the standards set out in Table 10, the results in Table 9 show that all nine test mixes resulted in a total charge passed either in the low or negligible range (with lower values/ranges being more favorable), well within acceptable standards for most projects depending on the intended use/conditions involved.

Table 10: Chloride Permeability Classifications for Concrete (*AASHTO, 1990)*

Chloride Permeability	Charge (coulomb)	Typical Concrete
High	>4000	High w/c ratio (>0.6)
Moderate	2000-4000	Moderate w/c ratio (0.4-0.5)
Low	1000-2000	Low w/c ratio (<0.4)
Very Low	100-1000	Latex-modified concrete, internally sealed concrete
Negligible	<100	Polymer infused/polymer concrete

Due to exceedingly low numbers throughout, it is hard to compare the changes in results from mix to mix, since most differences are within the range of statistical error. The summary statement for this study can still be made, however, that overall Type V portland cement and 15% silica powder performed best for Freeze-Thaw resistance and the Type I portland/GGBFS blend and 0% silica powder were best for chloride ion resistance. However, it should be noted that these results are not in any way based off of any statistical trends, and simply show how unpredictable the results to changes of UHPC mixes can be.

Additionally, while some differences may look exceptionally large, in relation to limits and typical values, all test results are incredibly low, and therefore all UHPC mix combinations tested would be perfectly suitable in regards to durability properties for almost any project. This includes J3, which uses a Type I/GGGBS cement mixture and 0% silica powder.

2.3 Corrosion

As evident throughout Section 2.2, there is extensive research into many areas of UHPC durability. However, the reaction of bridge decks with previously corroded reinforcing steel to partial or full depth repairs using UHPC is a very different story, being almost completely unmarked territory. Even Graybeal (2006, 2007) only mentions corrosion of UHPC in regards to surface corrosion of steel fibers on and near the exterior of the concrete, calling it “more aptly described as surface staining”.

The primary reasoning behind the concern raised by Floyd and Volz (2018) over the likelihood of UHPC bridge deck fills leading to further corrosion issues in the existing steel is the anodic ring phenomenon, or “Halo Effect”. The Halo Effect experienced by steel reinforcing in concrete is generally the result of the accelerated corrosion of steel in the base material that has come into contact with fresh concrete due to the very high pH in fresh concrete as compared to concrete that has been in use for an extended period of time.

This specific kind of corrosion cell is more specifically called macrocell corrosion. Steel rebar corrosion occurs due to an oxidation process that breaks down the passive film covering steel rebar in the presence of chloride ions or carbon oxide (Jones, 1996). That is to say, when an

anode and a cathode are separated from each other, the concrete itself acts as an electrolyte solution and a macrocell is produced. According to Hansson (2006), a simplified definition can be used, which states that macrocell corrosion in steel rebar is when an actively corroded bar is coupled to a passive bar or one of lower corrosion rate. Coupling being either direct contact or simply being in close proximity to, since the concrete is acting as a electrolyte solution that connects the two closely located reinforcing bars. Differences in corrosion states can occur due to differences in compositions (like the use of different sizes or grades of rebar in the same section of concrete) or differences in environments (like having rebar that goes through base concrete and the repair concrete). In these scenarios, the corroded bar becomes the anode and the passive bar becomes the cathode.

This is all in comparison to microcell corrosion, which does not need a specific scenario to occur, only an anode and cathode present directly adjacent to one another, which is simply caused by having surface irregularities, which is true of all steel reinforcing. This means that microcell corrosion occurs across every steel reinforcing bar on its own to varying degrees. Because of this, only macrocell corrosion, not microcell corrosion, will be studied in this thesis research, since this is the type of corrosion that indicates negative interaction between base concrete and repair material through the Halo Effect.

It should be noted that typically, fresh concrete has a pH of around 13, with concrete that has been allowed to age and experience carbonation from contact with the air having a pH of about 8. The high starting pH of typical concrete is mostly due to calcium hydroxide, which is a by-product of cement hydration. However, no research has been done to find the exact pH of UHPC,

in the fresh state or long-term state. It can be assumed that the low w/c ratio of UHPC that leads to often having large amounts of unhydrated cement within its densely packed matrix would be beneficial, lowering the pH of fresh UHPC. On the other hand, the fact that UHPC also starts with such a higher level of cementitious product compared to normal concrete, having no course aggregate (instead filling its voids with replacement cementitious materials such as silica fume), may be working against this and in fact increasing the pH of UHPC. This research, while not testing the pH of UHPC specifically, does hope to achieve results from small-scale Halo Effect/macrocell corrosion testing that indicate how UHPC acts as a repair material in comparison to normal concrete and other repair materials, which should give light to the overall effect on steel rebar, as well as the ph, of UHPC both in the fresh and long-term states.

Though no studies are currently available detailing how steel rebar reacts to UHPC as a repair material, a starting place for analysis is still necessary. Chosen here is the 2006 study "Macrocell and microcell corrosion of steel in ordinary Portland cement and high performance concretes" by C.M. Hansson, which looks at the corrosion performance of different concrete mixes based solely on their own. This study chose to look at three concrete mixes, one normal Portland cement mix and two high performance concrete (HPC) mixes (one using 25% cement replacement of blast furnace slag and one with 25% replacement of class C fly ash) as detailed in Table 11. In this study, seven 279 mm x 152 mm x 114 mm prisms were tested for each mix, totaling to 21 specimens, each containing three 10M reinforcing bars, one with a 25 mm cover from the top and two with a 25 mm cover from the bottom. These small scale specimens were cured with wet burlap for 7 days, stored outdoors for 5 months to prepare them for exposure to chlorides, and then tested for macrocell corrosion.

Table 11: Hansson (2006) Study Mix Designs in kg/ m^3

	Type 10 Portland Cement	Type 10SF Portland Cement	Slag	Fly Ash	Sand	Stone (20 mm)	Water (l)
Portland Cement	335	-	-	-	770	1,070	153
HPC- Slag	-	337	113	-	718	1,065	158
HPC- Fly Ash	-	337	-	113	718	1,065	158

For macrocell corrosion testing, the specimens were prepared for measurements as follows: coating the vertical surfaces with epoxy resin to prevent the access of oxygen into these surfaces, mounting a ponding well onto the top surface, connecting the bottom two bars to each other and finally, connecting the two bottom bars to the top bar through a 100 ohm resistor. From there, the ponding well was filled with a 3% NaCl solution off and on for two week periods for a total of 180 weeks, with the voltage drop across the resistor of each specimen being measured daily. The macrocell corrosion current between the top (anode) bar and the bottom (cathode) bars was determined using the measured voltage drops and Ohm's law for conversion. Overall, this study showed the HPC's as performing significantly better at protecting the steel rebar from macrocell corrosion than normal Portland concrete, having no active corrosion after 180 weeks in either HPC mix. In comparison, the Portland cement concrete mix experienced corrosion initiation as soon as 35 days into testing. This is almost certainly due to the fact that HPC, like UHPC, has a low permeability, and if no chloride ions can penetrate into the HPC specimens, there can be no electrical difference across the different levels steel reinforcing.

This result does not, however, guarantee that UHPC will still produce such a satisfactory result when used as a repair material. The impenetrability of UHPC may in fact cause more chloride ion build up in the base concrete, creating a large macrocell current across any steel rebar that goes through both materials. This likelihood, and how detrimental its impact may be, will be the focus of the corrosion portion of this study.

3.0 Mix Designs and Mixing Procedures

This section will detail the mix designs and mixing procedures to be used throughout this study, as well as the overall scope of work for the project. All research took place at Donald G. Fears Structural Engineering Laboratory, unless stated otherwise.

3.1 Scope of Work

Durability and corrosion testing were performed on the local alternative J3, as well on some comparison materials, including the commercially available UHPC mix Ductal® and a typical ODOT Class AA mix. These tests included chloride ion penetration, freeze-thaw, and scaling resistance testing to better understand the permeability of each mix.

In addition, both small- and large-scale corrosion testing was performed on these three mix designs, as well as a specialty bridge deck repair material Phoscrete, as requested by ODOT. Phoscrete is known for its durability properties because it is a high early strength MALP (Magnesium-Alumino-Liquid-Phosphate) concrete, which claims to stop rust on contact (by converting iron oxide to metal phosphate), resist chloride attack, and resist shrinking and cracking even under severe conditions. Although, Phoscrete is even more expensive than Ductal®, and past studies have shown similar Magnesium-Phosphate products to have disappointing freeze-thaw resistance (Cervo and Schokker, 2008).

The results from these tests provided great insight into the viability of J3 as a bridge deck repair material, both directly through the J3 results and by comparison to the results of the other mix designs.

3.2 Mix Designs

Detailed in Tables 12-14 is the mix design for the UHPC local alternative, J3, as well as that of the Ductal® and ODOT Class AA concrete mixes that were used as comparisons in both durability and corrosion testing.

Notes:

- The only change made to J3 for this testing is the use of densified silica fume instead of the undensified silica fume used in the original McDaniel (2017) study. This change was made because densified silica fume is more common and easier to transport, since the increased density means packaging can be smaller. This change does result in longer mix times, due to the mix needing longer to "break over" (change from all powder to a liquid state while mixing), but should not significantly change any other mixture properties.
- The original J3 mix was also designed to use completely oven-dried fine masonry sand, but this has been found to be impractical for large-scale field projects, and therefore the J3 mix design used for this project was modified for the use of normally-saturated (air dried) fine masonry sand. The specifics of this change are discussed further in Section 3.3.

- HRWR and AEA are standard concrete admixtures and stand for high range water reducer and air entraining admixture, respectively.
- The Phoscrete mix design is not listed because it comes in a premixed set consisting of only two components, liquid activator and dry mix, mixed in equal parts.

Table 12: J3 Mix Design

Material	Amount
Type I Cement (lb/yd^3)	1,179.6
GGBFS (lb/yd^3)	589.8
Silica Fume (lb/yd^3)	196.6
0.5 in. Steel Fibers (lb/yd^3)	255.2
Fine Masonry Sand (lb/yd^3)	1966
Water (lb/yd^3)	393.2
HRWR (fl. oz/yd^3)	24
w/c	0.2

Table 13: ODOT Class AA Mix Design

Material	Amount
Type 1 Cement (lb/yd^3)	588.0
#57 Crushed Stone (lb/yd^3)	1,841.0
Fine Aggregate (lb/yd^3)	1,281.0
Water (lb/yd^3)	232.0
HRWR (fl. oz/yd^3)	3.0
AEA (fl. oz/yd^3)	0.7
w/c	0.37

Table 14: Ductal® Mix Design

Material	Amount
Premix (lb/yd^3)	3,700.0
Water (lb/yd^3)	202.3
Premia 150 (lb/yd^3)	50.6
0.5 in. Steel Fibers (lb/yd^3)	262.9

Figure 2 shows the 0.5 in. steel fibers used in both the J3 and Ductal® mix designs.



Figure 2: 0.5 in. Steel Fibers

3.3 Mixing and Curing

The ODOT Class AA mixing procedure followed the ASTM C192 standard for normal weight concrete (NWC), with a few modifications made due to the fact that a large, stand-up mixer had to be used for the quantity of concrete made at one time. The specific mixer used throughout was a MIX 21:DD RH. First, the mixing drum was "buttered" with a small amount of sand, cement, and water to reduce moisture loss of the concrete from absorption by the mixer. The resulting slush was dumped prior to adding the proportioned mixture. Next, the coarse aggregate and a portion of the water were placed in the mixer until a slight shimmer could be seen on all surfaces of the aggregate. Finally, the mixer was started and the fine aggregate, cement, and water were put into the mixer, in that order, and mixed for a total of ten minutes. A constant ten minute mixing time was used instead of the normal three-three-two mixing pattern used for standard concrete to assure that the mix was thoroughly combined before use, without having to stop the large mixer, which could not be restarted after the addition of all of the concrete ingredients.

J3, being a UHPC mix design, requires a special high-shear mixing procedure, very different from that used for the ODOT Class AA mix. The procedure used for this testing usually includes the following: blending all dry constituents 5-10 minutes until fully combined, adding water and half of the HRWR over the course of 2 minutes, mixing all of the ingredients for 2 minutes, adding the second half of the HRWR over 1 minute, mixing all ingredients again for 5 minutes, and finally, adding fibers and continue to mix until fibers are evenly dispersed in the mixture. However, due to the use of saturated sand, which had a 10% moisture content, 10% additional sand by weight was added, and the equivalent weight of water was taken out. At the time mixing

would normally be completed, the mix was not fully saturated or "broken over" and therefore some of this water that was taken out, along with some additional HRWR, was added back in and mixed for an additional 5 minutes. An example of the J3 UHPC alternative before "break over" and at the end of mixing can be seen in Figures 3 and 4. In addition to J3, the Ductal® mix used for comparison was also prepared using the high shear mixing procedure detailed above. The main differences for the Ductal® mix being that the dry constituents come already pre-mixed, and that it took over 60 minutes to reach Ductal's® "break over" point, but no additional water was added, only an additional small portion of HRWR.



Figure 3: J3 before "Break Over"



Figure 4: J3 after "Break Over"

After all mixing procedures, except for Phoscrete which had no need to be finished, all specimens were cast into their appropriate molds for each test, finished with a (wetted) trowel, and cured according to the curing procedures outlined in the following sections. All curing procedures are variations on ambient air curing methods, because as described in Sections 2.2.1 and 2.2.2, though ambient air curing is the most vulnerable to durability issues, it is also the most reflective of what to expect in the field, and specimens should still produce more than adequate results no matter the curing method. Additionally, if the results are indeed sufficient for this curing method, they would only improve using other curing methods. Photographs of all of the cast specimens are shown in Figures 5-8.

It should also be noted here that for the ODOT AA mix, all specimens were properly rodded and tamped in accordance to ASTM C192, with most specimens being consolidated with a large vibrator to assure proper consolidation of specimens such as the large corrosion joints. None of the other mixes needed to be consolidated using the same measures because they are all considered to be self-consolidating.



(a) *(b)*

Figure 5: First Half of Small-Scale Corrosion Specimens



Figure 6: AA Large-Scale Corrosion Specimen (left) and Durability Specimens (right)



Figure 7: Ductal® Large-Scale Corrosion Specimen (left) and Durability Specimens (right)



Figure 8: J3 Durability Specimens (left) and Phoscrete Durability Specimens (right)

3.4 Mixture Compressive Strengths

The 28-day compressive strengths for all mixes used within this study are shown in Table 15. These compressive strengths were all determined in accordance with ASTM C39-18.

Table 15: Concrete Compressive Strengths Summary

Concrete Type	Average Compressive Strength (psi)
ODOT AA for Small-Scale Corrosion Specimen First Halves	5,620
All other ODOT AA	6,560
J3	18,560
Ductal®	23,850
Phoscrete	6,100

4.0 Chloride Ion Penetration, Freeze-Thaw Cycling, and Scaling Resistance Testing

This section outlines the testing procedure and results of the chloride ion penetration testing, freeze-thaw cycling, and scaling resistance testing of the ODOT Class AA, Ductal®, and J3 concrete mixes.

4.1 Chloride Ion Penetration

4.1.1 Introduction

Rapid Chloride Ion Permeability (RCIP) testing was conducted on all three mixes detailed in Section 3.1 using ASTM C1202-17 standards. RCIP testing is extremely important for understanding permeability across different concrete types, and should definitively show the advantages of UHPC over conventional concrete in regards to durability.

However, it should be stated that there is a common misconception that RCIP is a direct test of permeability, which it is not. RCIP testing measures the bulk flow of chloride ions through a specimen, not a specific type of ion movement/how the ions flow through the specimen, meaning it is only appropriate for comparing the overall permeability of different concrete mixes to one another.

4.1.2 Procedure

For this testing, at least three specimens were tested for each mix design at both 28 and 90 days of age. All specimens were moist cured using wet burlap and plastic until the specimens were ready to be demolded, at which point they were put into a lime water bath until one day before testing. All specimens were cut from the top and bottom of two 4 in. x 8 in. (100 mm x 200 mm) cylinders into 2 in. thick slices, so a total of 12 cylinders were cast, 4 for each mix. Slices were cut using a water-cooled diamond saw blade and slice surfaces were ground flat where needed. Testing was accomplished by passing a 60 V potential difference across each slice and measuring the amount of electrical current that passes through the specimen in a 6 hour period. During testing one side of each specimen was immersed in a 3% NaCl solution, with the other side being immersed in a 0.3 N NaOH solution. Both the 3% by mass NaCl solution and the 0.3 N NaOH solution were made using deionized water and laboratory grade dry 32 reagents. Ultimately this meant using 12 grams of NaOH per 1000 mL of water and 31 grams of NaCl per 1000 mL of water. Testing conditions were achieved using a RCIP testing machine by Germann Instruments and a computer software program called PROOVE'it.

At any point during testing, if any of the specimens or their solutions exceeded a temperature of 90°F, that test was ended immediately, with its time of termination noted and a rating of high chloride ion penetrability given. This was done to protect the testing cell and to prevent evaporation of the testing liquids.

One day before testing, specimens were placed in a vacuum desiccator with a pump system capable of maintaining vacuum pressure of less than 50-mm Hg. The vacuum pump was run on the dry specimens for 3 hours before pumping deionized water in and running the vacuum desiccators for another hour with the specimens completely submerged. After this, the pump was turned off and left sealed for 18 hours, at which time testing could begin. The pump system used is shown in Figure 9.



Figure 9: Vacuum Pump (right) and Desiccator (left)

There is some debate on the viability of this testing procedure, due to the fact that the high voltage applied leads to high temperatures, which in turn increase the total charge passed through the specimens. Additionally, when measuring the total charge passed the test actually measures all of the ions passing through the specimen, not just the chloride ions. However, since UHPC should be incredibly impermeable, over-estimation is not a large concern, so this testing set-up was determined to be adequate for the purpose of this thesis research.

Note that for the first round of chloride ion testing specimens were cast as they would be in the field. This meant the inclusion of the 0.5 in. steel fibers that give Ductal® and J3 their exceptional tensile strength. Due to this inclusion, however, passageways were opened up in both J3 and Ductal® that disrupted the accuracy and short-circuited the testing. To get an accurate reading of the permeability of the UHPC mixtures, two new cylinders were cast for both J3 and Ductal® without fibers so that new specimens could be made in the same manner as the original specimens, with an additional slice cut out of the center of each cylinder to make a total of three specimens for both 28 and 90 day testing. Only the results from the second round of testing are presented in Section 4.1.4.

4.1.3 Testing

The test set-up used throughout testing is shown below in Figure 10.

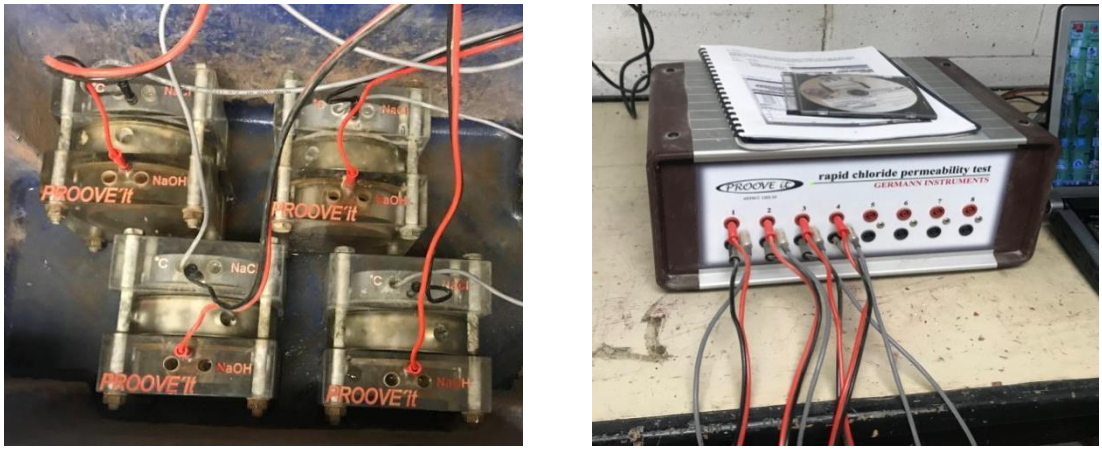

(a) (b)

Figure 10: Chloride Ion Permeability Testing Using PROOVE'it- Typical

The visual state of the test specimens after 28 day testing are shown in Figure 11 to show how much surface corrosion occurred for each mix design due to testing, with minimal surface corrosion occurring on the ODOT AA specimens and little to no surface corrosion occurring on the Ductal® and J3 specimens.

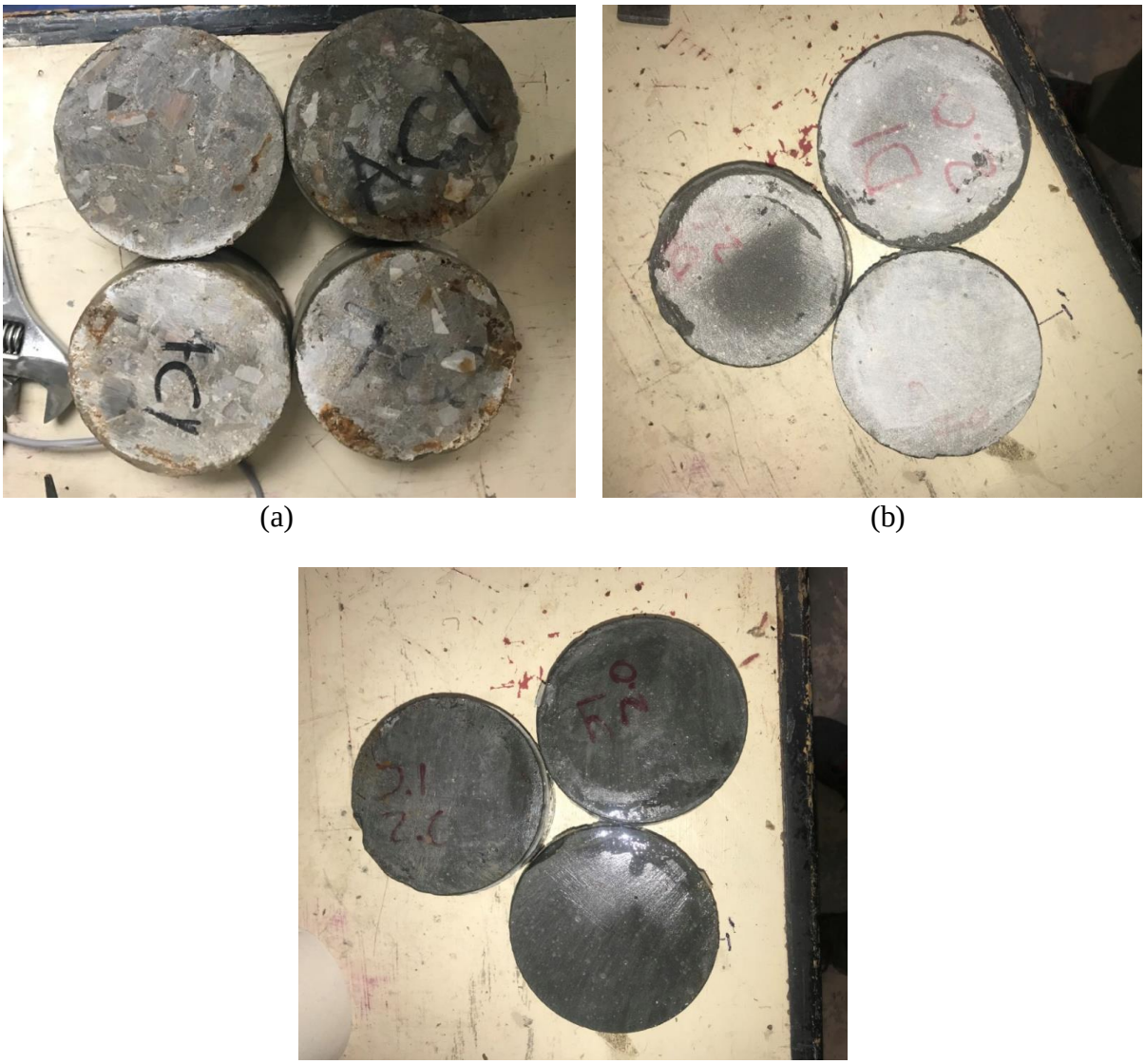

(a) (b)

(c)

Figure 11: State of Chloride Ion Penetration Testing Specimens After 28 Day Testing for (a) ODOT AA (b) Ductal® (c) J3

4.1.4 Summary of Results

The average coulombs passed for each set of specimens and the corresponding permeability class for each mix at both 28 and 90 day testing are presented in Tables 16 and 17, with the rating system for chloride permeability presented as Table 18. Note that a concrete mix with a lower chloride permeability class is considered more resistant to chloride attack, and therefore more favorable, than one with a high chloride permeability class.

Table 16: Chloride Ion Permeability Testing Results- 28 Days

	AA	J3	Ductal®
Average Coulombs Passed	2463.50	251.00	60.67
Chloride Permeability Class	Moderate	Very Low	Negligible

Table 17: Chloride Ion Permeability Testing Results- 90 Days

	AA	J3	Ductal®
Average Coulombs Passed	1831.50	62.50	27.50
Chloride Permeability Class	Low	Negligible	Negligible

Table 18: Chloride Permeability Classifications for Concrete

Chloride Permeability Class	Charge (Coulomb)
High	>4000
Moderate	2000-4000
Low	1000-2000
Very Low	100-1000
Negligible	<100

Ultimately, all results found for chloride ion testing were as expected. The ODOT AA had moderate average permeability, right within the range of what is normal and acceptable for a standard concrete mix that is to be used in non-highly corrosive environments. Both J3 and Ductal® had quite low average permeability, a result that is also in line with what one would expect based on past studies into UHPC and given the nature of UHPC's dense particle matrix, which works by having very little open space (air pockets) for water or ions to flow through. The decrease in permeability that occurred for all three mixes between 28 and 90 day testing is also as expected, due to the fact that the specimens continued to cure (and therefore continued to hydrate and gain strength) during this period, albeit at a significantly lesser rate than between initial set and 28 days of testing.

4.2 Freeze-Thaw Cycling

4.2.1 Introduction

Freeze-thaw testing was conducted to test the durability resistance of each mix when exposed to harsh winter conditions.

4.2.2 Procedure

Freeze-thaw testing was done in accordance to ASTM C666-15 Procedure A (freezing and thawing in water). A total of ten specimens were tested, three for each of the three mixes detailed in Section 3.1, and one control ODOT AA specimen, which was connected to a temperature probe to monitor the temperature change inside the machine. All freeze-thaw specimens were 4 in. x 4 in. x 15 in. ASTM C666-15 Procedure A was chosen for freeze-thaw testing because it simulates a more aggressive environment and is easily achievable by the equipment available at the University of Oklahoma Fears laboratory.

For this procedure, specimens were moist cured for 14 days prior to testing, first using wet burlap, followed by soaking in a lime water bath as soon as the specimens could be demolded, before finally being placed in a freezing-and-thawing apparatus for testing. During cycling, all specimens were completely surrounded by a layer of water 1/8 in. thick. This was achieved by wrapping each specimen with two coated wires, each 1/8 in. thick, which were also used to help lift the specimens out of their encasements when they needed to be examined. A total of 350

cycles were performed for each specimen, with each cycle taking roughly 4 hours. This number of cycles was chosen because although only 300 cycles are required by the ASTM procedure, it was shown by Chumping (2015) that a significant change in data can occur around 300 cycles for this testing approach, so while unlikely, data was collected past 300 cycles to ensure no drastic changes occurred that meant the specimens needed to be studied for an extended period of time past the required 300 cycles.

Each cycle consisted of two parts, which lowered the temperature from 40 to 0°F and then raised the temperature back from 0 to 40°F, respectively. Freeze-thaw cycling was started from the thaw temperature (40°F), and anytime freeze-thaw cycling needed to be paused, all specimens were kept in a frozen state. Note that at any point in the cycling, if a specimen was found to have reached the Freeze-Thaw failure criteria, i.e. RDM of less than 60%, the specimen would have been removed from testing and a dummy specimen would have replaced it within the testing apparatus for consistency. It was highly unlikely that any of the UHPC specimens would have come anywhere near these failure criteria, but there was a small chance for the conventional concrete mix (ODOT AA) to experience failure, so all specimens were closely monitored for this unlikely scenario, though it never occurred during this set of testing.

At intervals not exceeding 36 cycles, specimens were thoroughly thawed and placed in a lime water bath for 24 hours to prevent moisture loss and prepare the specimens for testing. Soaking for at least 24 hours was essential for all of the specimens to be of the same moisture level whenever they were tested.

Only RDM values of each specimen were taken throughout testing. These values were calculated by measuring the fundamental longitudinal (transverse) frequency and dividing it by the original fundamental longitudinal (transverse) frequency for each specimen. This results in RDM in the form of a percentage, where 100% is the starting point of the internal structure of the specimen, and deterioration results in ever decreasing values.

These frequencies were measured with a frequency meter called an Emodumeter, which works by creating a mechanical impact with a small metal ball on one side of a specimen and measuring how long it takes for the vibrations to be felt by a sensor located on the other end of the specimen. This type of measurement is effective because it indicates the internal structure of the specimen (i.e., if a large amount of microcracks are present, it will take longer for the impact to be felt). The decision to only measure RDM was made because while RDM can be unreliable (due to ambient air curing methods resulting in high levels of un-hydrated cement in UHPC, as discussed in Section 2.2), mass loss and length change can be even more unpredictable, changing dramatically with any moisture level change. Figure 12 shows a specimen being tested in the Emodumeter while Figures 13 and 14 show a typical transverse frequency initial measurement and resulting final output, respectively.



Figure 12: Freeze-Thaw Specimen in Testing Machine

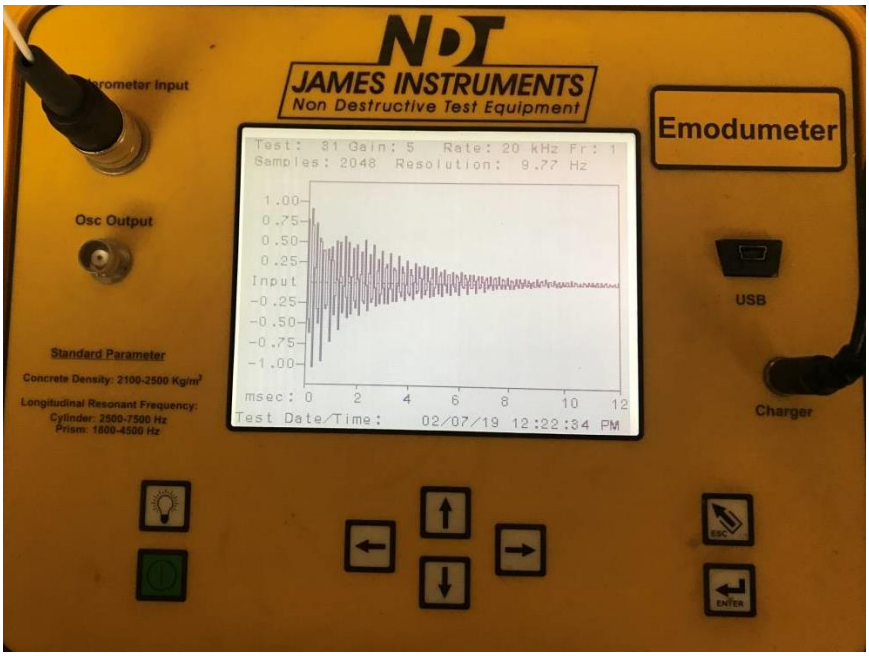

Figure 13: Typical Emodumeter Transverse Frequency Measurement

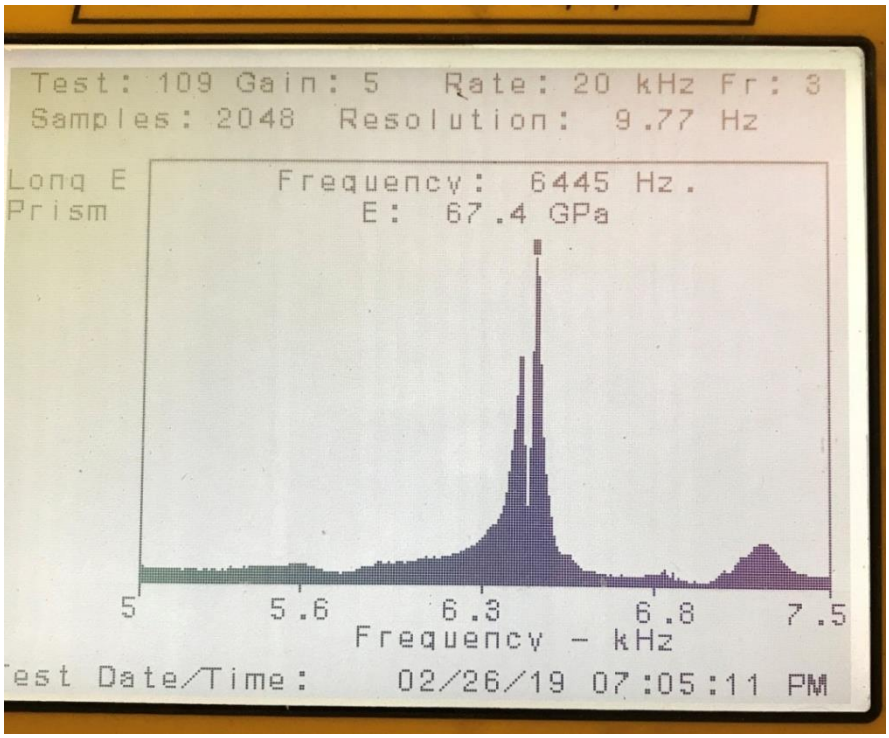

Figure 14: Typical Emodumeter Transverse Frequency Output Page

Following the guidelines in ASTM C666-15 and ASTM C215-14, the Emodumeter data collection device was set to collect 2048 points per test with a sampling rate of 20 kHz. Additionally, all specimens were tested three times during each round of testing, and their frequencies averaged together. All data points more than 10% apart from the average were rejected and recollected.

After each round of testing the freezing-and-thawing apparatus was rinsed out and all containers were refilled with fresh water. Specimens were then put back into the freezing-and-thawing apparatus in a new location, so that each specimen experienced the conditions of all parts of the apparatus and no one specimen was continuously subject to harsher conditions than another.

4.2.3 Testing

The freeze-thaw specimens prior to testing are shown in Figures 15 and 16. All specimens had limited surface deterioration at this point in testing, and their starting frequencies were recorded to be used as the original value for finding each specimen's RDM values throughout testing.



Figure 15: Freeze-Thaw Specimens in the Testing Chamber- Cycle 0



Figure 16: Condition of All Freeze-Thaw Specimens- Cycle 0

As evident in Figure 17, after 350 cycles significant deterioration of the ODOT AA specimens could be seen, including chipping of edges and wearing away of the surface to the point of coarse aggregate showing through.



Figure 17: Deteriorated State of an AA Freeze-Thaw Specimen- Cycle 350

Figures 18 and 19 show that the Ductal® and J3 specimens show significantly less deterioration, with only small holes forming along their surfaces for the majority. The exception being a singular hole that formed between cycle 285 and cycle 315 in Specimen D1 (as seen in Figure 20) which triggered a spike in RDM for the specimen due to water now being able to penetrate farther into the specimen and hydrate more of the unhydrated cementitious materials within the specimen.

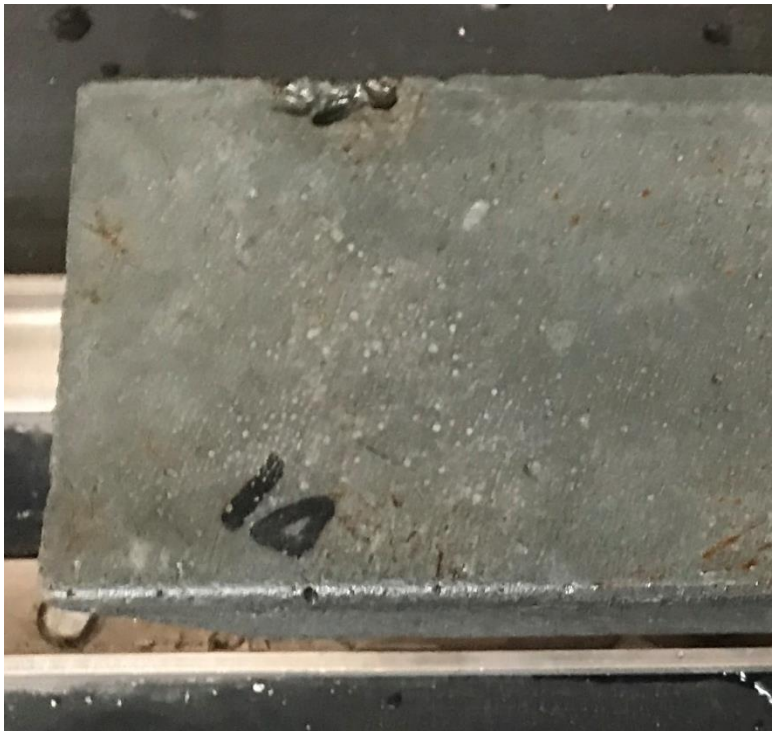

Figure 18: Deteriorated State of a Ductal® Freeze-Thaw Specimen- Cycle 350



Figure 19: Deteriorated State of a J3 Freeze-Thaw Specimen- Cycle 350



Figure 20: Hole Formed on the Side of Ductal® Freeze-Thaw Specimen- Cycle 315

However, though the Ductal® specimens only experienced the expected minimum amount of surface spalling, each of the three Ductal® specimens did experience a significant amount of surface corrosion of the steel reinforcing fibers on all four sides of each specimen, as shown Figure 21. At the conclusion of testing, all three J3 specimens had also begun to show this kind of surface corrosion of fibers, but to a significantly lesser extent. This is significant because very similar corrosion patterns were seen by Ductal® and J3 in scaling testing, as discussed in Sections 4.3.3 and 4.3.4, and could be indicative of J3 having better fiber suspension during concrete setting. It should be noted, however, that surface corrosion of fibers is expected for UHPC structures in highly abrasive environments like those simulated by freeze-thaw cycling and scaling resistance testing, and in no way affects the overall strength or durability of the UHPC. This is unlike the corrosion of internal reinforcing bars through contact with concrete, UHPC or otherwise, which is extremely detrimental to the strength and durability of the structure and is therefore the focus of Chapter 5. Instead, how well a specimen withstood freeze-thaw cycling is determined by the state of its internal structure, as represented by final RDM values.



Figure 21: Surface Corrosion of Ductal® Freeze-Thaw Specimen- Cycle 350

4.2.4 Summary of Results

The average RDM values for the different concrete mixtures at 350 cycles are presented in Table 19. Additionally, a graph of the average RDM values over the course of all 350 cycles is presented as Figure 22. From these values it can be seen that a small amount of internal deterioration occurred to the ODOT AA specimens, indicated by a small decrease in RDM, to a final average value of 99%. It should be noted that this value is still much better than that seen by other typical concrete mixes, and certainly well above the failure criteria of 60%. Both of the UHPC mixtures, on the other hand, show a slight increase in RDM. This seemingly strange phenomenon is explained by the presence of unhydrated cementitious particles in the specimens prior to testing becoming more and more saturated as testing progressed due to more and more

surface openings occurring in the specimens that water could then penetrate into. This is consistent with the results and explanation given by both the Graybeal (2007) and Ahlborn (2011) studies discussed in Section 2.2.2, which also showed significant average RDM increases for ambient air cured UHPC specimens, with final average RDM values of 110% and 102% respectively.

Table 19: Freeze-Thaw Testing Results

Average RDM at 350 Cycles (%)		
AA	J3	Ductal®
99.1	103.1	102.5

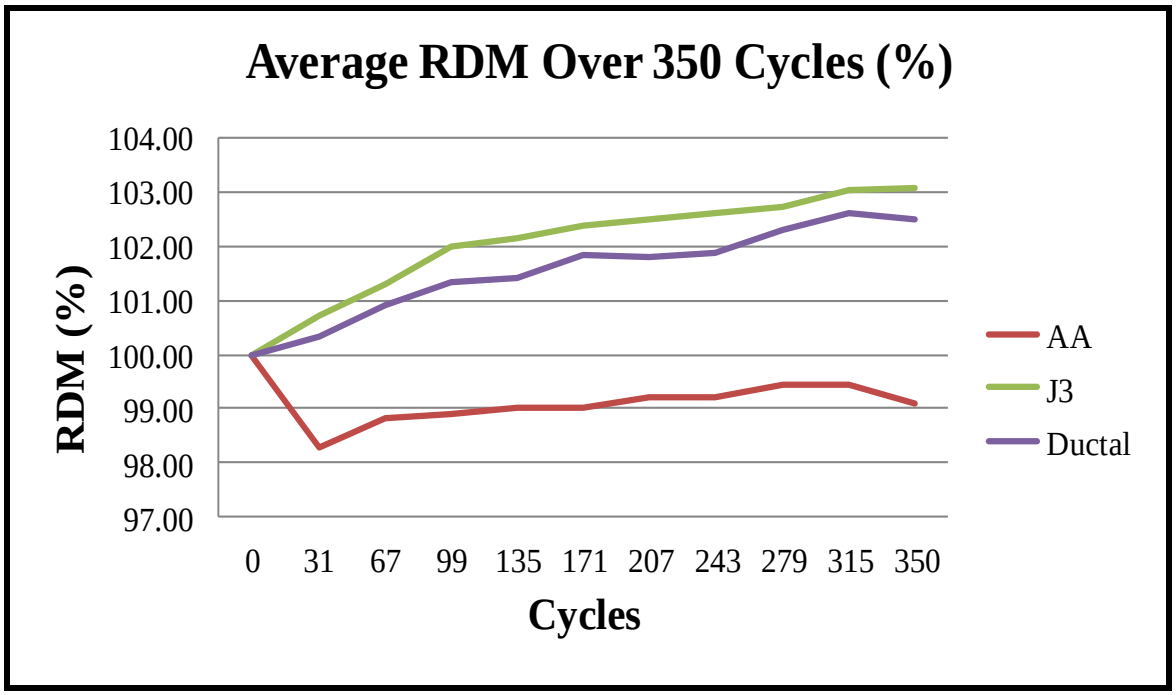

Figure 22: Average RDM Values Over 350 Cycles of Freeze-Thaw Testing

However, as was noted by Graybeal (2007), these large RDM values do not guarantee that the internal structures of the UHPC specimens are responding well. In fact, large RDM values only mean that particle saturation is occurring, which at an excessively high rate could actually be a sign of a weak internal structure that allows for the easy passage of water.

This leaves assessment of the external structure as the only other means of measuring the response of these mixtures to freeze-thaw cycling. As visible in Figure 18 in Section 4.2.3, the AA mixtures began to experience noticeable deterioration towards the end of testing, as was expected for this testing set-up. This included significant pocketing of the specimen surfaces and even some large aggregate beginning to show through. None of the specimens for either UHPC mixture were anywhere close to this level of deterioration, with only light pocketing and surface corrosion of steel reinforcing fibers occurring. This decisively low level of deterioration is again very much expected for UHPC under freeze-thaw conditions. In conjunction with the reasonable RDM values obtained and discussed previously, these results are enough to indicate that both J3 and Ductal® would perform well under similar conditions in the field.

4.3 Scaling Resistance

4.3.1 Introduction

Scaling resistance testing was conducted to test the permeability of each mix when experiencing harsh winter conditions with the addition of deicing chemicals.

4.3.2 Procedure

Scaling resistance was tested in accordance to ASTM C672-12 using two specimens for each of the UHPC mix designs, J3 and Ductal®, and two for the conventional ODOT Class AA concrete mix, for a total of 6 specimens. All scaling specimens were 9 in. x 15 in. x 2 in. Scaling resistance testing was done after 28 total days of curing: 14 days of moist curing, done in the same fashion as that of the freeze-thaw specimens, and 14 days of ambient air curing, in accordance to ASTM 672-12. This testing was conducted by first covering each specimen with a ¼ in. layer of a calcium chloride and water solution containing 4 g of calcium chloride to each 100 mL of solution. Each specimen had a 1 in. x 1 in. foam boarder epoxied all the way around its outside edge prior to testing to act as a container for the testing solution, as shown in Figure 23.

From there, each specimen was put through 50 cycles, where one cycle involved going from 0°F for 16-18 hours to 40°F for 6-8 hours in an environmental chamber. The environmental chamber used was located in S11 of the Carson Engineering Facility located on the University of

Oklahoma's main campus. One cycle was completed daily, with water added when necessary to maintain proper depth of solution. The surface of each specimen was properly flushed at the end of every fifth cycle. If tests needed to be paused for any reason, specimens were kept frozen. At 25 cycles and at the end of testing, all specimens were visually examined using the surface condition rating system in ASTM 672-12, as detailed in Table 20. Note that the bottom horizontal surface for each specimen was used as the testing surface for scaling due to its consistent finish. This choice was also key for this study in particular because in practice the top surfaces of Ductal® specimens are always ground off because something within the Ductal® proprietary mix (likely a de-foaming agent) causes all excess air to rise to the surface as large air pockets. However, by using the bottom surfaces for testing, this unusual surface condition could play no part on Ductal® scaling resistance results.

Table 20: Scaling Surface Condition Rating System in Accordance with ASTM C672

Rating	Condition
0	No scaling
1	Very slight scaling (3 mm [1⁄8 in.] depth, max, no coarse aggregate visible)
2	Slight to moderate scaling
3	Moderate scaling (some coarse aggregate visible)
4	Moderate to severe scaling
5	Severe scaling (coarse aggregate visible over entire surface)

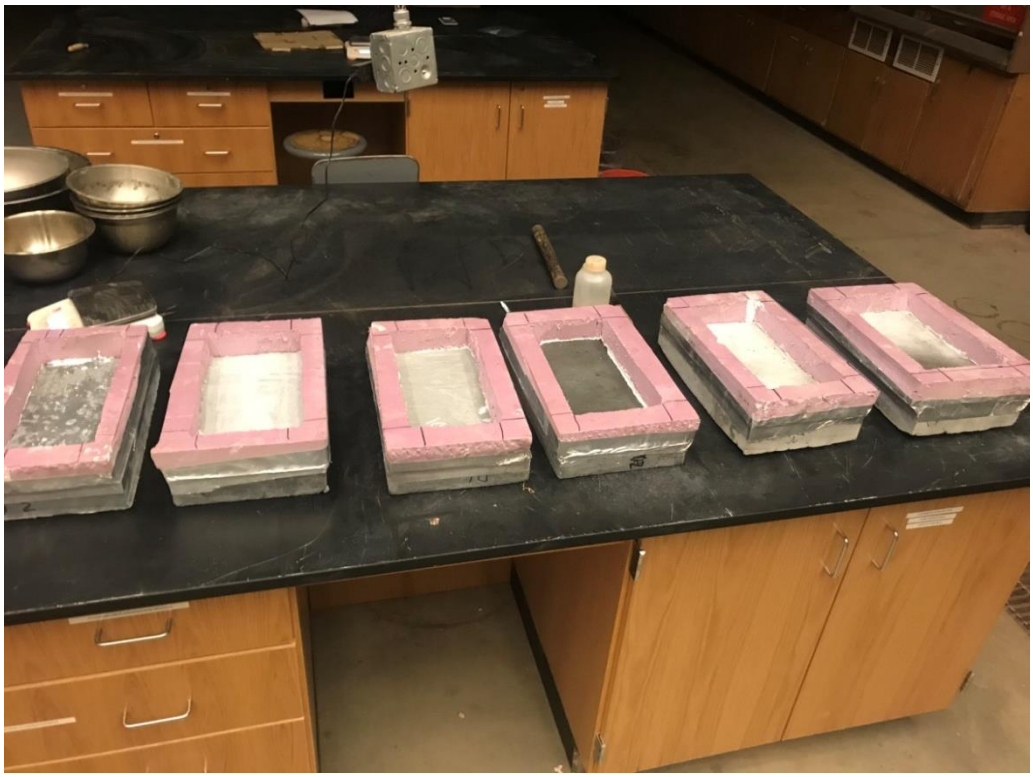

Figure 23: Condition of Scaling Specimens- Cycle 0

4.3.3 Testing

After 7 cycles, slight pockets could be observed on the surface of both of the ODOT AA specimens; though none of the J3 or Ductal® specimens showed any signs of visible deterioration at this stage of testing.

At 25 cycles, both ODOT AA specimens had significant pocketing, as shown in Figure 24, almost to the point of exposing coarse aggregate in select places, with a majority to all of their surface area showing signs of dusting. Also at this point during testing, one of the Ductal® specimens (D1), shown in Figure 25, began to show significant visual signs of corrosion of the

steel fibers along its exposed surface, with slight dusting and pocketing visible. Little to no dusting or pocketing, as well as limited surface corrosion, was observed on the other Ductal® specimen or either of the J3 specimens.

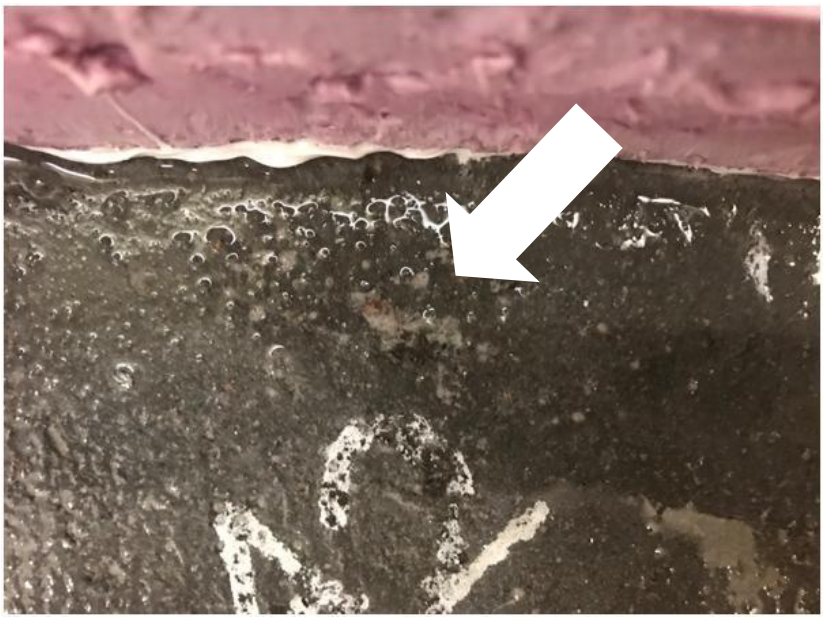

Figure 24: Visual Pocketing on AA Specimen- 25 Cycles



Figure 25: Visual Corrosion of Steel Fibers on Ductal® Specimen- 25 Cycles

At 50 cycles, the specimens were in the states shown in Figure 26. Since 25 cycles, the pocketing of both of the ODOT AA specimens had increased a considerable amount, and pocketing had begun to occur on specimen D1, as shown in Figures 27 and 28, respectively. Dusting of the entire surface was also noted for each of these three specimens during this period of cycling, with the other Ductal® specimen, D2, experiencing dusting of almost its entire surface as well. No substantial dusting or pitting occurred on either of the J3 specimens, with the final state being almost completely unchanged, as shown in Figure 26(c).



(a)

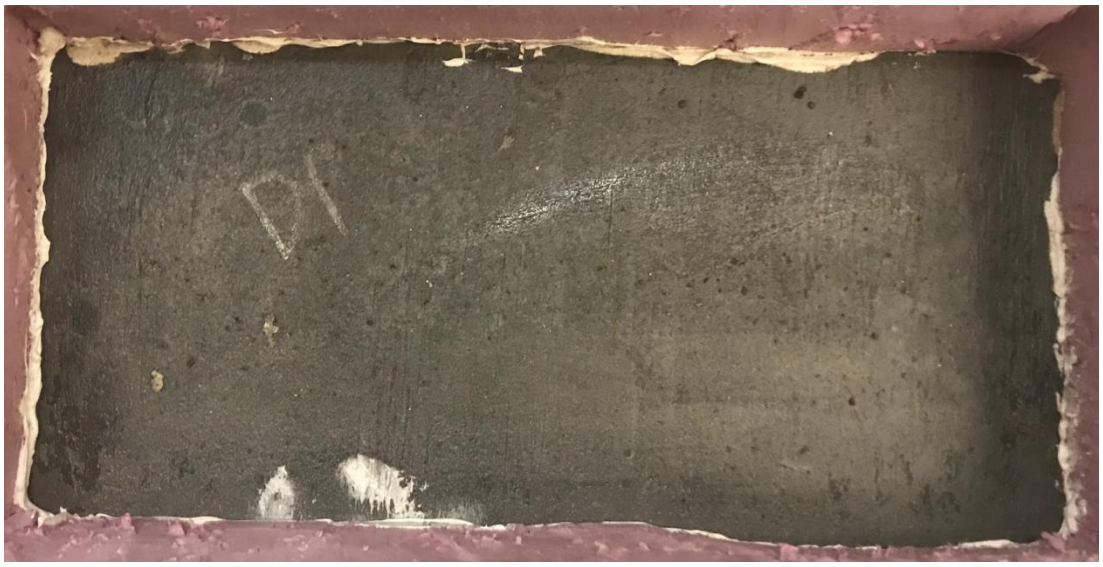

(b)



(c)

Figure 26: Visual Examination of Scaling Specimen at 50 Days for (a) ODOT AA (b) Ductal® (c) J3



Figure 27: Progression of Visual Pocketing on AA Specimen- 50 Cycles

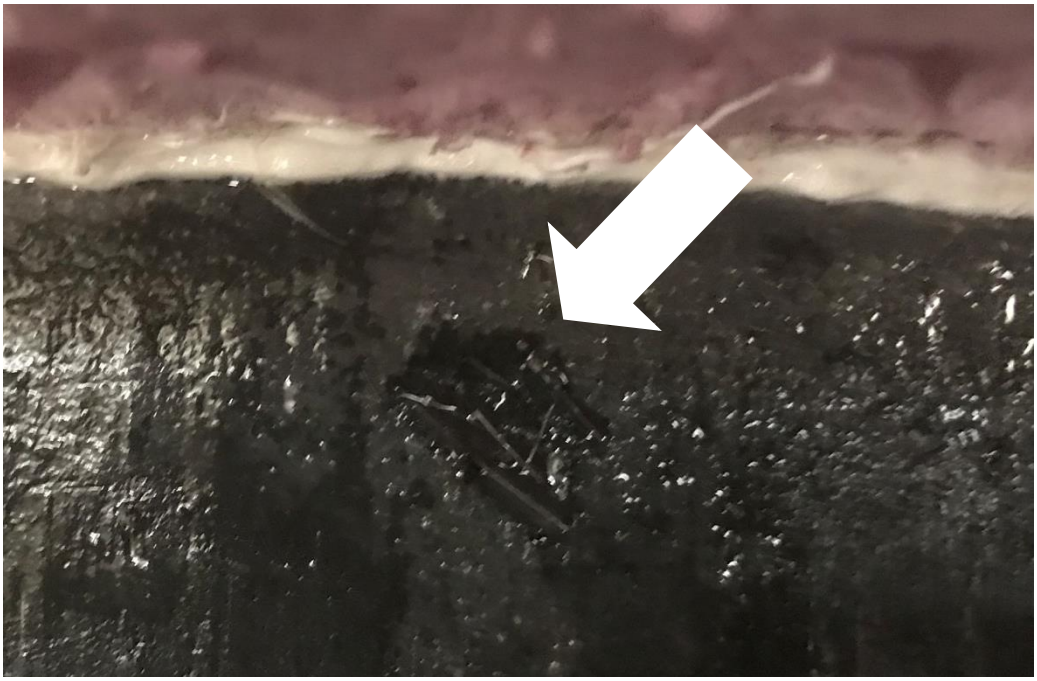

Figure 28: Visual Pocketing on Ductal® Specimen- 50 Cycles

4.3.4 Summary of Results

Visual ratings were given to each specimen at 25 and 50 cycles based on the states of the specimen surfaces, as examined in Section 4.3.3 through Figures 24-28, and are presented in Table 21.

Table 21: Average Scaling Visual Rating Results

	25 Cycles	50 Cycles
AA1	1.00	1.50
AA2	1.50	2.00
Average	1.25	1.75
J1	0.00	0.00
J2	0.00	0.00
Average	0.00	0.00
D1	0.75	1.50
D2	0.25	1.00
Average	0.50	1.25

Assessment based on these ratings show that both ODOT AA specimens performed as expected, with significant deterioration occurring due to a large amount of both dusting and pocketing of the surface, while both J3 specimens performed exceedingly well, with no substantial dusting or scaling occurring at any point during testing. Ductal®, on the other hand, had two specimens that performed very differently, with one experienced similar levels of deterioration as that of the ODOT AA specimens, while the other specimen experienced a large amount of dusting but significantly less pocketing. Despite the large difference in deterioration levels, however, these

responses still combined to give Ductal® an average final rating much higher than expected, especially compared to that of J3.

5.0 Corrosion Testing

This section outlines the testing procedure and results of both small- and large-scale corrosion testing of the ODOT Class AA, Ductal®, J3, and Phoscrete concrete mixes.

5.1 Introduction

To obtain the most accurate understanding of the effects of a UHPC repair joint on reinforcing steel with previous corrosion, the ideal situation would be to test slabs that have been in active use. Therefore, the University of Oklahoma research team worked in conjunction with ODOT to identify and procure slab sections with existing corrosion that had been previously removed from service. These specimens were then retrofitted with a joint made of one of the four test mixes specified in Section 3.1 and subsequently corroded in an accelerated test setup to produce valuable insight on the comparative corrosion protection capabilities of each mix through visual examination. This was what was referred to as "large-scale" corrosion testing. In addition, "small-scale" corrosion testing was performed to specifically measure the macrocell outputs, or "Halo Effect", of each of the four mixes when used as a repair material.

It is important to note here the two distinct types of reinforcing steel corrosion that could occur as a result of this corrosion testing: pitting and surficial (Jones, 1996). Pitting corrosion occurs when corrosion becomes concentrated, burrowing itself into the steel, and shows visually as dark spots of corrosion intermittently placed across the reinforcing steel's surface. Surficial corrosion, on the other hand, occurs as a light in color, uniform coating of corrosion across the surface of the steel reinforcing. This kind of surface corrosion is much more likely to stick to the concrete

surrounding it because it is in direct and constant contact with the concrete. Neither type of corrosion is necessarily more severe than the other, both being quite harmful for the steel reinforcing; however, the "Halo Effect" is typically evident in a concrete repair by the presence of surficial corrosion of the reinforcing steel in the substrate (original) concrete and not of the reinforcing steel within the repair material. However, this is not always the case, and this kind of corrosion is often much harder to identify, since most of the surface corrosion is pulled away when the concrete is removed for visual examination. Therefore, care was taken to identify all levels and kinds of corrosion (as applicable and feasible), since any indication of corrosion could be a sign of the "Halo Effect" at work.

5.2 Small-Scale Corrosion Testing

5.2.1 Procedure

Specific testing for the Halo Effect was accomplished on small scale composite specimens using an ODOT Class AA base concrete in conjunction with a Ductal®, J3, ODOT AA, or Phoscrete "repair". This testing focused on macrocell corrosion, because that is the type of corrosion that is indicative of the "Halo Effect" (i.e., corrosion only due to the contact of the two different materials). Microcell corrosion, despite being known to be the main contributor of corrosion of steel reinforcing, can be assumed to occur throughout all reinforcing, regardless of what type of concrete it is within, or whether that concrete is old or new. Therefore, microcell corrosion would not provide any information on the interaction of old concrete and repair material and was not measured in this testing.

The composite specimens used for this part of the corrosion testing were 24 in. x 12 in. x 3 in., with each specimen consisting of half base concrete and half repair material. The base concrete halves included the addition of NaCl at dosage rates of 0, 4, and 8% by weight of cement, to represent base concrete of differing levels of corrosion and previous chloride ion penetration. This method of having NaCl directly in the base concrete is more effective and direct than the ponding method employed by other studies for macrocell corrosion testing. This meant a total of 12 specimens were cast, three for each repair mix and three for the normal 0% NaCl ODOT class AA mix, which acted as a control. Each set of halves were cast one at a time (base concrete followed by repair material), cured for 28 days, and contained three No. 3 bars with electrical wiring soldered to each end, ultimately extending out of the top of the two different concrete halves. After the second 28 day curing time, each bar had its two halves electrically coupled via a 100 ohm resister to allow the measurement of the voltage drop across each bar every couple of days, similar to the set-up of the Hansson (2006) study discussed in Section 2.3. Specimens were cured using a standard 7 days of wet curing and 21 days of air curing for both sets of curing times.

Although the base concrete already contained varying levels of NaCl, specimens were also placed in a 5% NaCl solution, with the water level 0.5 in. below the top of the specimens, to prevent any damage to the electrical wiring coming out of the specimens. This was done to allow for easier passage of ions through the different concrete halves while also accelerating the corrosion within the specimens. The small-scale corrosion molds and testing set-up are shown in Figures 29 and 30, respectively.



(a) (b)

Figure 29: Small-Scale Corrosion Specimen Molds

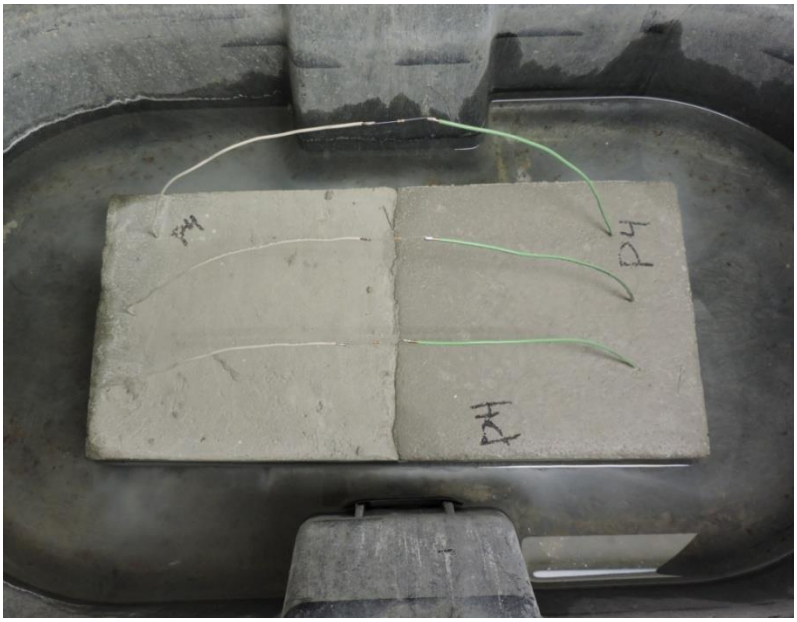

Figure 30: Typical Small-Scale Corrosion Testing Set-Up

Though not a direct measurement of overall corrosion as a whole, these macrocell readings can be used to compare the specific effect of different repair materials on the corrosion of steel rebar in base concrete. Macrocell current corrosion testing was done for a total of 10 weeks, after which the steel rebar was exposed in the 4% and 8% NaCl specimens for visual examination.

The 0% specimens were left in their testing chambers and allowed to continue to corrode for an extended period of time past the reach of this study. Using the visual examinations and the macrocell measurements it was possible to determine if UHPC, and more specifically the mix design J3, accelerated the corrosion process more or less than a typical bridge joint repair

5.2.2 Testing

After a week of testing, the Ductal® small-scale corrosion specimen containing 0% NaCl, D0, began to show signs of corrosion at the joint, unlike anything seen in any of the other 11 specimens, as shown in Figure 31. By week two, all of the Ductal® specimens began to show signs of corrosion. The second and third specimens, however, showed signs of corrosion not through the obvious patching seen on D0, but through corrosion spotting, as shown in Figure 32. None of the other small-scale specimens experienced any signs of surface corrosion directly at the joint between the two materials, in either of these forms, only experiencing light coloration around their edges where they were in contact with the 5% NaCl solution. Additionally, during large-scale corrosion testing, a similar type of corrosion as that of D0 occurred along the Ductal® specimen joint. This will be further discussed in Section 5.3.3.

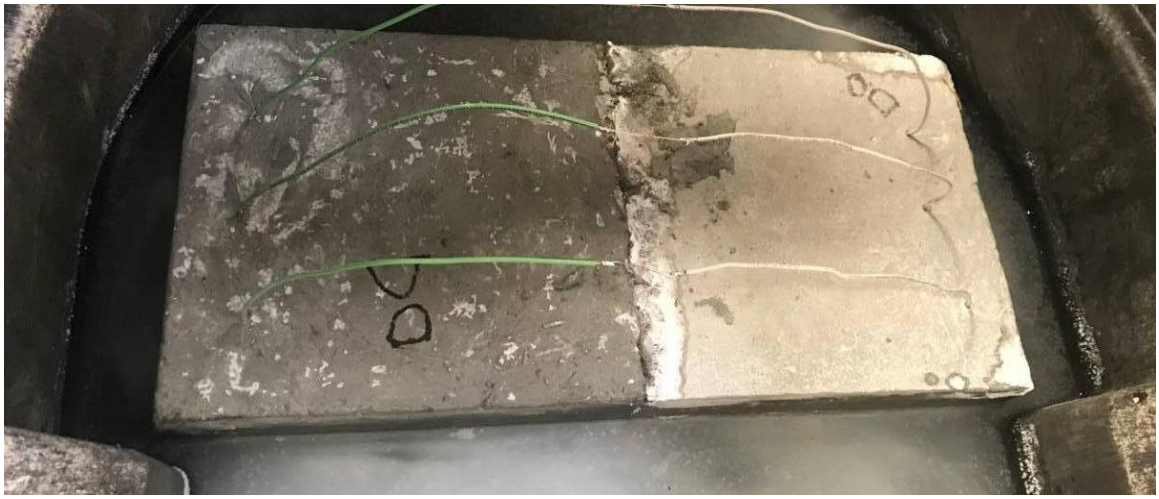

Figure 31: Joint Corrosion in Ductal® Small-Scale Corrosion Testing Specimen- Patching



Figure 32: Joint Corrosion in Ductal® Small-Scale Corrosion Testing Specimen- Corrosion Spotting

Ultimately, no measurable macrocell currents formed across any of the reinforcing bars in any of the specimens during the duration of this testing. This was due to insufficient amounts of corrosion across the reinforcing bars to induce a current that could travel across the two types of concrete that made up each specimen, despite the high levels of NaCl present in most specimens. This was a good sign for all of the concrete mixtures, since the presence of a measurable macrocell current would have indicated an immense amount of corrosion forming across the steel reinforcing on both sides of the bars.

Though no macrocell current values can be reported, the joints of the 4% and 8% NaCl specimens were chipped away to give some comparison of corrosion response of the four different repair materials, as discussed in the rest of this section and shown in Figures 34-37.

Additionally, a photograph of the type of steel rebar put into these specimens before testing is presented as Figure 33 so that the difference between the typical amount and type of corrosion present on a piece of steel rebar before and after testing can be made clear. This difference is made most clear by the darker color and distinct starting location of the active corrosion (after testing). It is assumed in this testing that all previous surface corrosion was purely superficial and would have come off completely during either casting or chipping, and all actual surficial or pitting corrosion due to testing conditions would have occurred with or without the initial presence of this light surface corrosion.



Figure 33: Steel Rebar Before Testing- Typical

As illustrated in Figures 35 and 36, the excavation of the Ductal® and J3 specimens that contained 4% and 8% NaCl in their base concrete revealed minor pitting corrosion on a majority of their reinforcing bars, all congregated at the joint, with some traces of this pitting also forming on the base concrete side. Similarly but to a higher degree, excavation of the ODOT AA specimens revealed significant pitting corrosion on all of its reinforcing bars, starting exactly along the line of the joint and moving along the original ODOT AA (base) concrete side, almost to the point of complete coverage (Figure 34). This kind of corrosion happening only in the base material is exactly what could be expected of these specimens from the "Halo Effect" given the time period of testing.

Unlike the expected and characteristic results of the other three materials, however, excavation of the Phoscrete specimens revealed significant amounts of pitting corrosion along the repair material side, with the 8% NaCl specimen also exhibiting a visible layer of surficial corrosion completely covering the reinforcing steel along the base concrete side (Figure 37). This is highly unanticipated, given that the one of the main purposes of Phoscrete as a repair material is to

prevent corrosion of the reinforcing steel (by converting iron oxide to metal phosphate, reportedly). This extreme reaction, as well as Phoscrete's response during the large-scale corrosion testing discussed in Section 5.3.2, raises concern about the durability and corrosive resistant properties of Phoscrete where there was little concern previously. Therefore, additional testing should be done on Phoscrete to assess its durability and corrosion properties to fully understand its viability in the field.



(a) (b)

Figure 34: Corrosion State of Rebar Reinforcing at Joint of AA Small-Scale Corrosion Specimens with (a) 4% NaCl (b) 8% NaCl



(a) (b)

Figure 35: Corrosion State of Rebar Reinforcing at Joint of J3 Small-Scale Corrosion Specimens with (a) 4% NaCl (b) 8% NaCl



(a) (b)

Figure 36: Corrosion State of Rebar Reinforcing at Joint of Ductal® Small-Scale Corrosion Specimens with (a) 4% NaCl (b) 8% NaCl



(a) (b)

Figure 37: Corrosion State of Rebar Reinforcing at Joint of Phoscrete Small-Scale Corrosion Specimens with (a) 4% NaCl (b) 8% NaCl

5.2.3 Summary of Results

Ultimately, conclusions about the "Halo Effect" studied by the small-scale corrosion testing can only be made through visual examination, and therefore the adequacy of each of the concrete types can only be evaluated on a relative basis with each other. In this case, however, this is not a significant issue. This is because the main area of concern for this testing was simply the confirmation that the non-proprietary mix J3 would have an acceptable response to corrosion testing, the answer to which was made very clear through visual examination alone. Indeed, both J3 and Ductal® produced similar, acceptable results and out-performing the standard ODOT AA mixture that would be used in a simple bridge deck repair.

As a side note, while there were no voltages, and therefore no macrocell currents, formed across any of the reinforcing bars at the conclusion of this initial testing, there were small amounts of voltages measured between adjacent bars within each of the small-scale corrosion specimens. While these are not the readings that would indicate a macrocell forming due to the Halo Effect happening across the two different repair materials, the primary area of concern for this study, these readings do show a macrocell forming from just having bars adjacent to each other in each of these specimens. Since the 0% NaCl specimens were left in the prescribed testing conditions and allowed to continue to corrode, measurements were taken between each set of bars on both sides of each specimen to be used as a control set of data. Points 1-3 are on the original base material (ODOT AA) side and points 4-6 are on the repair material side, as labeled on Figure 67 in the Appendices. These measurements are to be compared to future values in subsequent studies to see if the use of any one repair material increases macrocell corrosion from having multiple bars in a specimen more rapidly than the other repair materials, and are reported in Table 22 in the Appendices for this use.

5.3 Large-Scale Corrosion Testing

5.3.1 Procedure

The retrofitting process for the large-scale joint specimens included: cutting the ODOT bridge slabs to an appropriate size (18 in. wide x 60 in. deep x 9 in. thick), chipping away 4 in. of the damaged concrete from the 18 in. width to expose the steel rebar, and casting a 5 in. x 60 in. x 9

in. repair replacement joint, producing a minimum 1 in. cover to the rebar exposed from the chipping process. The exposed No. 5 rebar layer revealed in each slab was connected together using a No. 5 longitudinal bar tied to the far ends of the exposed rebar sections. The longitudinal bar was placed on the top most layer of reinforcing when laid down flat, putting it closest to what ultimately became the finished surface, to allow for the needed wires to extend out of the top of the specimens. These electrical wires were soldered onto both ends of each connective longitudinal bar to allow for the DC power supplies to be connected after curing of the specimens, as discussed in the following paragraph. The slabs before and after chipping are shown in Figures 38 and 39, with Figure 40 showing the final rebar construction.



Figure 38: Joint Specimens before Chipping



Figure 39: Joint Specimens after Chipping



Figure 40: Joint Specimen Rebar Fully Tied Together

One joint specimen was cast for all four of the concrete mixes in this testing: ODOT AA, Ductal®, J3, and Phoscrete. Phoscrete was used in this corrosion testing because, as mentioned previously, this product is specifically intended to reduce the effects of steel corrosion in concrete repairs, but is previously untested by ODOT. After the joints were cast, moist cured for 7 days, and air cured for another 21 days, they were connected to a DC power supply capable of

supplying up to 3 A of current and submerged in a 5% NaCl solution to accelerate the reinforcing bar corrosion using electrochemical methods similar to Wang et al. (2014, 2017) and Abosrra et al. (2011). This was accomplished using large wooden containers lined with plastic with a 5% NaCl solution at a level 2 in. below the top of the specimens to prevent any damage to the electrical wiring extending out of the specimens, similar to the set up of the small-scale corrosion specimens. All of the wooden containers were given foam "feet" so that when the specimens were placed inside, they were elevated off the ground 1 in., allowing the testing solution to penetrate the bottom of the specimens.

From there, the testing set up followed the electrochemical method, which works by creating a complete circuit that runs through steel reinforcing (or similar conductive metals), which causes the steel reinforcing to release electrons, in turn oxidizing the steel reinforcing and corroding it. For this testing, the required complete circuit was achieved by using a stainless steel rod sitting in the NaCl solution as a cathode (as shown in Figure 41) and the longitudinal steel reinforcing rod in the repair material side of each specimen as the anode. From there, each specimen was connected using electrical wiring so that a 0.2 A current could flow continuously from the positive terminal of the power supply to the steel reinforcing, through the concrete and surrounding NaCl solution to steel rod, and ultimately back to the negative side of the power supply. This test set-up is shown in Figure 42.



Figure 41: Stainless Steel Rod and Electrical Wiring for Large-Scale Corrosion Testing

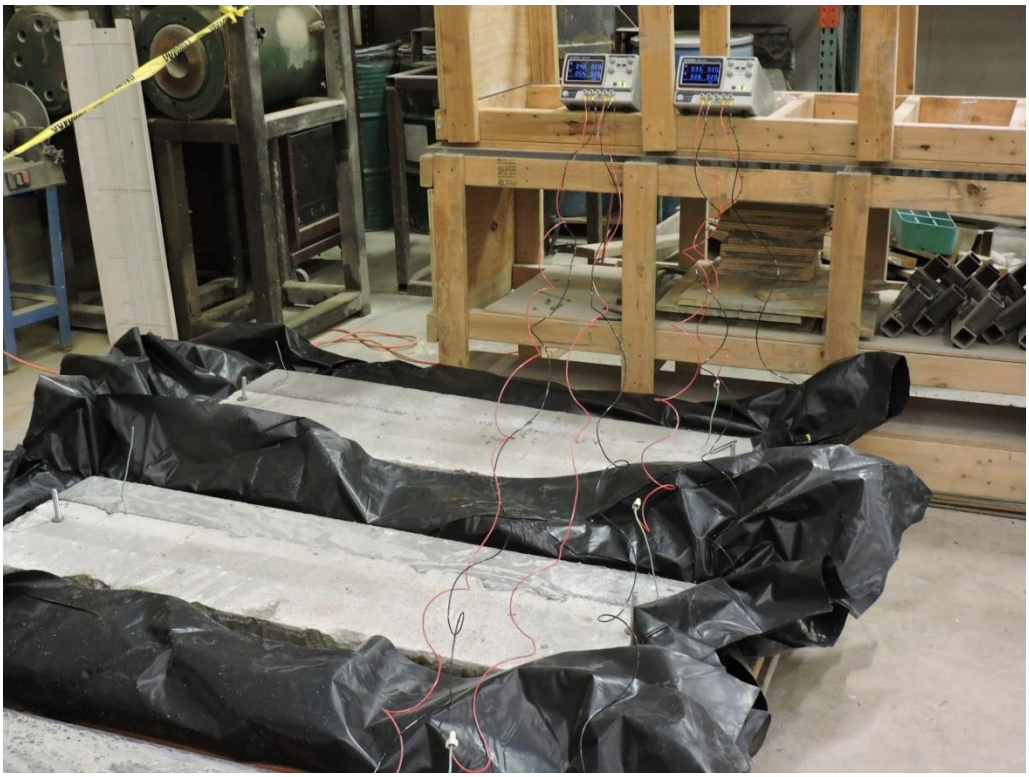

(a)



(b)

Figure 42: Large-Scale Corrosion Testing Set-up

After one week of supplying a current of 0.2 A through each specimen, the slabs were partially chipped back, starting from the side farthest from the input of the current, so that the first layer of vertical reinforcing could be visibly inspected for corrosion. From there, the slabs were chipped along each reinforcing bar layer by layer until a sufficient amount of corrosion could be observed. Once sufficient corrosion was achieved, chipping was done at the joint interface of each specimen along the same reinforcing bars as those chipped away previously. This was done to confirm if any corrosion had occurred between the base concrete and the repair material, and if so, which side(s) the corrosion occurred on. Once corrosion at the joint was confirmed, roughly ten weeks into the accelerated corrosion process, a final round of chipping was done along the joint, as close to the inflow of current as possible. This was done to observe the highest level of potential corrosion occurring within each specimen. Timing, location, and progression of corrosion were all closely documented for each of the slabs and are detailed in Section 5.3.2.

5.3.2 Testing

During the first week of testing, the water pools of each specimen began to fill with a coating of corrosion that had already begun to leech off, except for Phoscrete, which secreted a white film that has been previously unseen by work done in this laboratory. This film is present in Figure 43. After a week, the white film was covered with a corrosion film like the rest of the large-scale corrosion specimens. After two weeks of testing, the corrosion that was now in the water of all four specimens became great enough that it filled all of the testing water, but mostly occupied the bottom of the testing containers. This level of corrosion was maintained through to the end of testing and is shown in Figure 44.



Figure 43: White Film in Water of Large-Scale Corrosion Specimen- Phoscrete



Figure 44: Corrosion in Water of Large-Scale Corrosion Specimens- Typical

Also during the first week of testing, a corrosion spot along the joint of the Ductal® specimen began to form. By week two, this corrosion spot was in the state shown in Figure 45. This could have been due to a number of reasons relating to a poor joint-face connection between the Ductal® and the old AA concrete it was cast onto, but most likely it is due to the Halo Effect occurring rapidly along this joint. The justification for not assuming a simple poor joint-face connection being that previous Phase I testing showed that Ductal® possesses exceptional bond strength to substrate (base) concrete, and therefore a poor bond was unlikely in this scenario. From week three up until testing was concluded after 10 weeks, the surface corrosion along the Ductal® joint progressed at a steady and alarming rate, as shown in Figure 46. None of the other specimens showed any significant signs of surface corrosion during any point during testing, except along the anticipated reinforcing bar paths. This observation will be discussed more in Section 5.3.3.



Figure 45: Joint Corrosion in Ductal® Large-Scale Corrosion Testing Specimen- Week Two (Ductal® on left side of image)



Figure 46: Joint Corrosion in Ductal® Large-Scale Corrosion Specimen- Week Five

Though none of the other specimens experienced joint corrosion, a strange interaction did begin to occur at the joint of the Phoscrete specimen starting roughly 45 days (week 7) after corrosion testing began. A thick, dark green liquid began to form around the joint, similar to what leaked out and caused the white film in the surrounding solution in the first week of testing. The makeup and reasoning for this liquid forming are unknown, and no literature on Phoscrete

addresses if this is normal for a specimen in a highly corrosive environment. However, it is hypothesized that something in the chemical make-up of Phoscrete (which contains magnesium, aluminum, phosphate, and multiple other chemicals to try to help prevent corrosion and freeze-thaw damage) reacted with the NaCl in the surrounding solution, and at this point in the testing the solution had made its way far enough into the joint to begin to interact and produce the green substance shown in Figure 47.



Figure 47: Green Liquid in Joint of Phoscrete Large-Scale Corrosion Specimen- Week 7

Roughly 8 weeks into testing, the Ductal® specimen also began to produce a small amount of green liquid from its joint, however this liquid was much lighter in color than that seen on the Phoscrete specimen, and was accompanied by streams of white liquid that seem to trail down the

joint, as seen in Figure 48. It is hypothesized that this liquid was also a by-product of a chemical reaction occurring between the NaCl solution and the Ductal® mix. Due to its proprietary nature, there is no way to know for sure what compound within the Ductal® mix could have reacted, but two likely sources are a type of de-foaming agent (used to push out excess air during curing) or an unusual supplementary cementitious material.



(a) (b)

Figure 48: Green Liquid in Joint of Ductal® Large-Scale Corrosion Specimen- Week 8

Final states of these two unexpected chemical reactions happening at the surface are shown in Figures 49 and 50.



Figure 49: Green Liquid in Joint of Phoscrete Large-Scale Corrosion Specimen- Week 10



Figure 50: Green Liquid in Joint of Ductal® Large-Scale Corrosion Specimen- Week 10

After only one week of testing, the first sign of rebar corrosion was also visible on all specimens. As shown in Figure 51, a thick black liquid began to be produced out of the exposed ends of each specimen. Though no more than a few inches of liquid was ever formed on any one bar, and the amount of each rebar end that was completely corroded off due to the formation of this liquid was never significantly high, only reaching a maximum of 0.75 inches, this level of corrosion could still be cause for concern in the field. This is because the chemistry of steel rebar reacts so violently with NaCl and other corrosive solutions found in the field that 5 to 10 times the volume of fully corroded steel rebar is produced in actual corrosion during this expansion reaction. This becomes a problem in the field because if internal reinforcing were to experience this kind of corrosion, like that seen on the exposed rebar ends, it could generate large expansive forces that can crack and spall the concrete the reinforcing steel resides in. Fortunately, this level of corrosion of rebar ends is expected for this testing set-up, and the joint made with J3 did not exhibit any more of this corrosion than any of the other joints, often actually being less or right at the level of rebar end corrosion of the other joints. By the end of testing, the corrosion of the exposed rebar ends had reached the extent shown in Figure 52. Both Figure 51 and 52 are of the ODOT AA specimen, which was considered the control specimen.



(a) (b)

Figure 51: Visible Confirmation of Corrosion of Vertical Reinforcing Bars- Week 1



Figure 52: Typical Level of Corrosion at the Conclusion of Testing- Week 10

Figures 54-57 provide updates of the specimens over the 10 week testing period, while Figures 58-61 show each layer of reinforcing steel immediately after chipping. The last layer of steel reinforcing that was excavated and examined, after being completely removed from testing, chipped, and allowed to sit out in open air for 24 hours, is also presented as Figure 62. This is significant because with no forced current or surrounding NaCl solution, all reactions of this exposed reinforcing steel came only as a result from what had already occurred within the specimens, and all pitting corrosion that revealed itself was previously present in the steel reinforcing. Figure 53 is also used as a guide to show the order in which the layers were chipped away, as is referenced throughout the rest of this section and Section 5.3.3.



Figure 53: Chipping Sequence of Large-Scale Corrosion Specimens

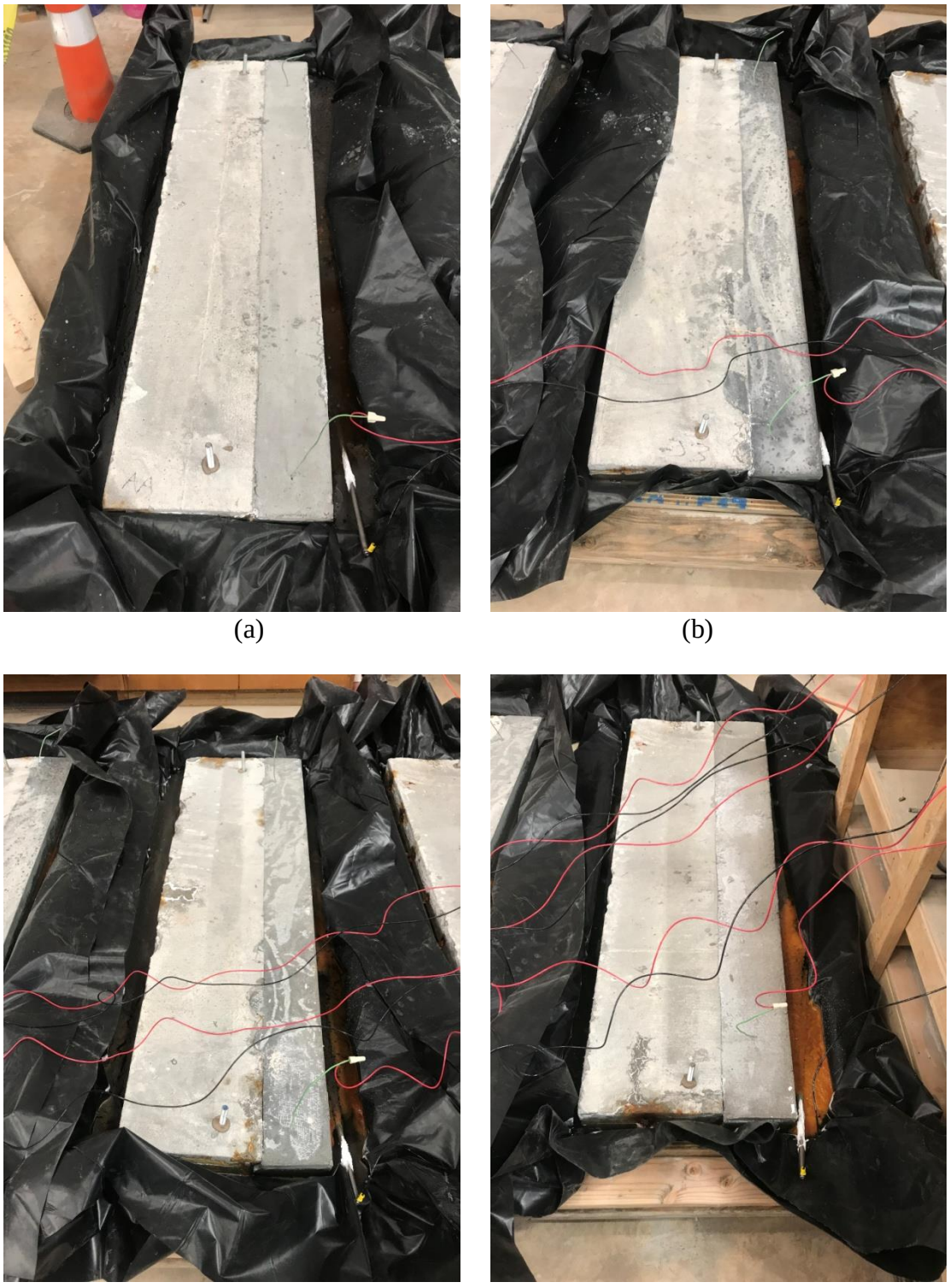

(a) (b)

(c) (d)

Figure 54: Week 1 Update of Large-Scale Corrosion Specimens Using (a) ODOT AA (b) J3 (c) Ductal® (d) Phoscrete

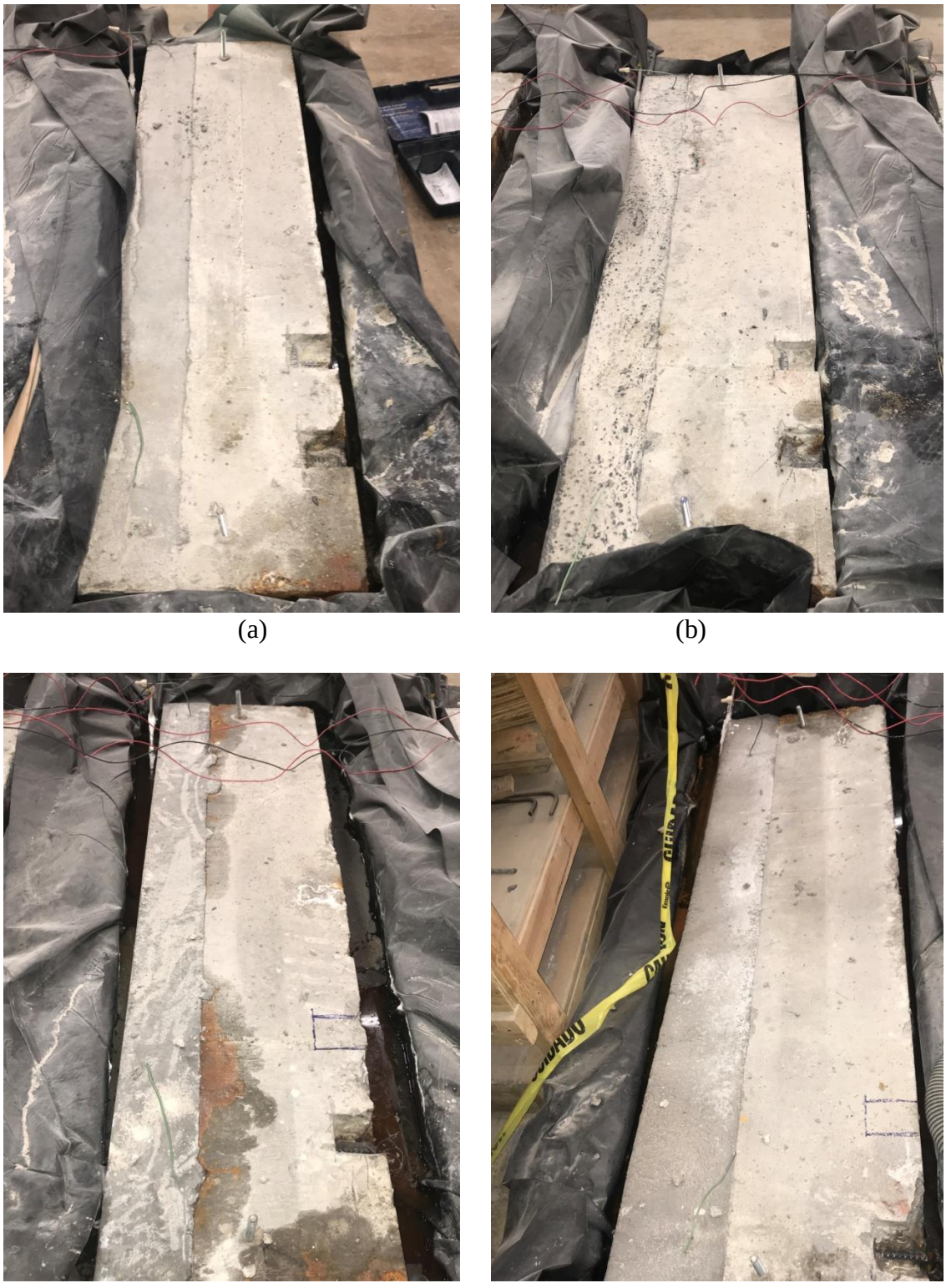

(a) (b)

(c) (d)

Figure 55: Week 3 Update of Large-Scale Corrosion Specimens Using (a) ODOT AA (b) J3 (c) Ductal® (d) Phoscrete

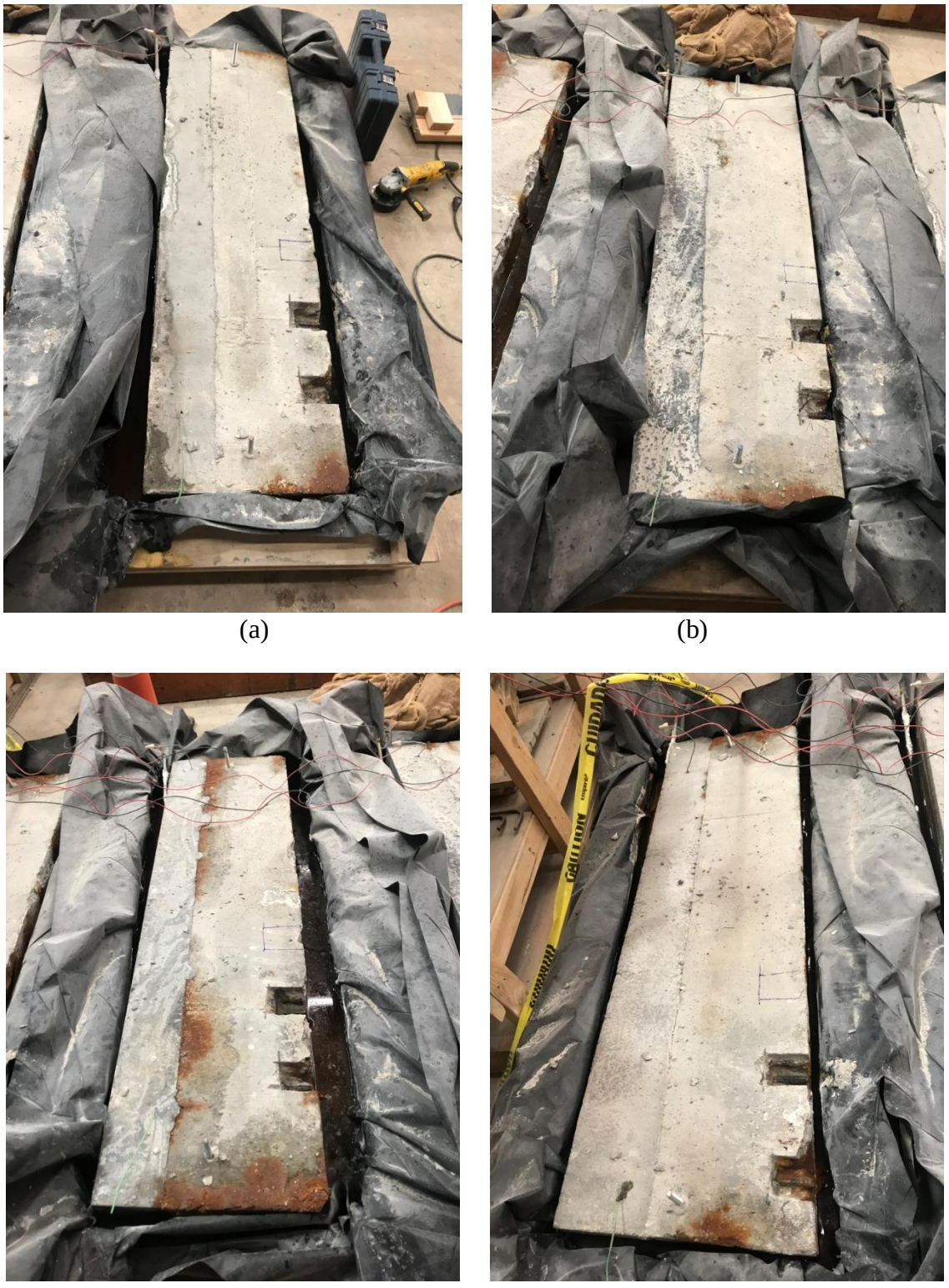

(a) (b)

(c) (d)

Figure 56: Week 6 Update of Large-Scale Corrosion Specimens Using (a) ODOT AA (b) J3 (c) Ductal® (d) Phoscrete

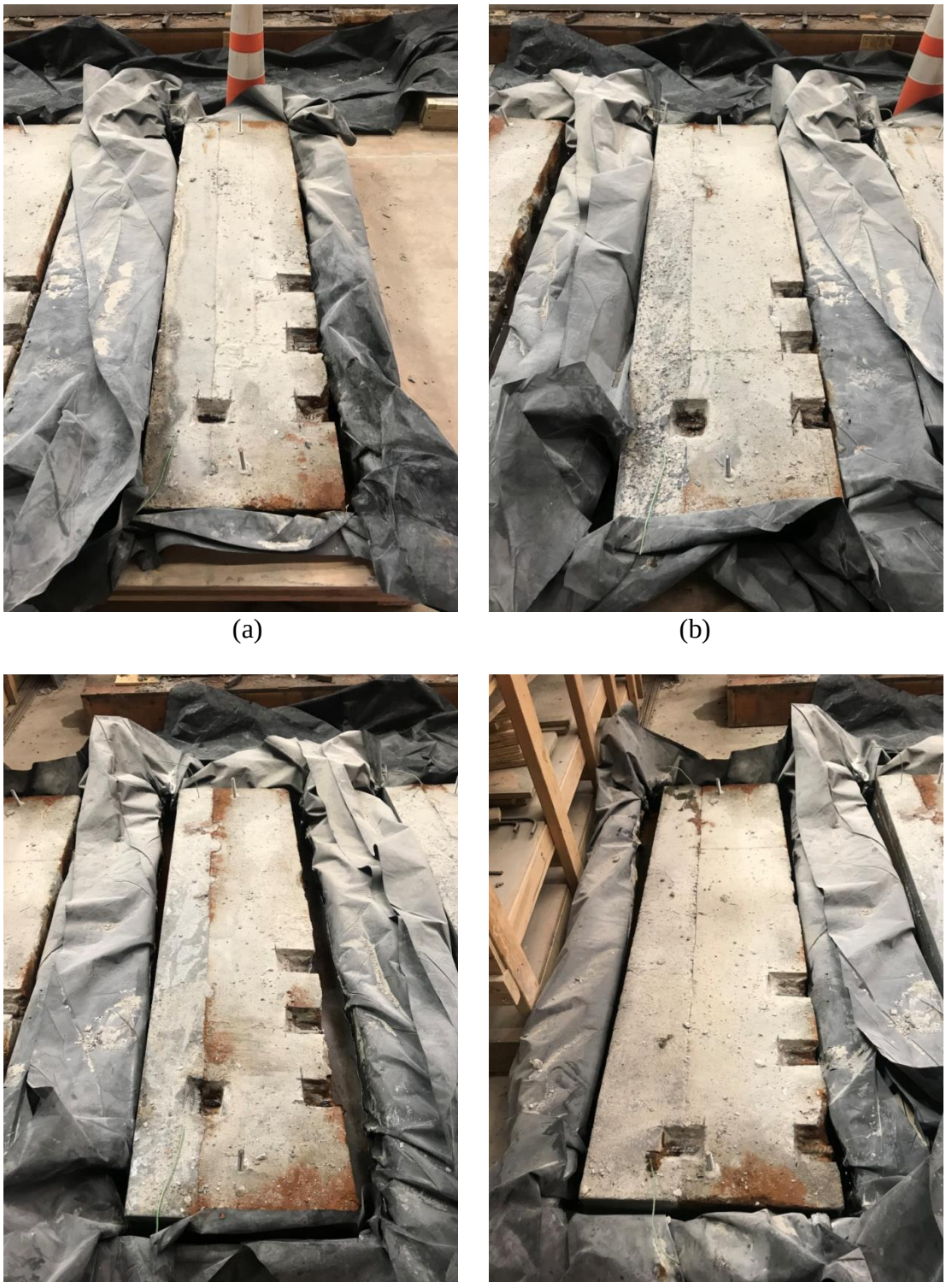

(a) (b)

(c) (d)

Figure 57: Week 10 Update of Large-Scale Corrosion Specimens Using (a) ODOT AA (b) J3 (c) Ductal® (d) Phoscrete

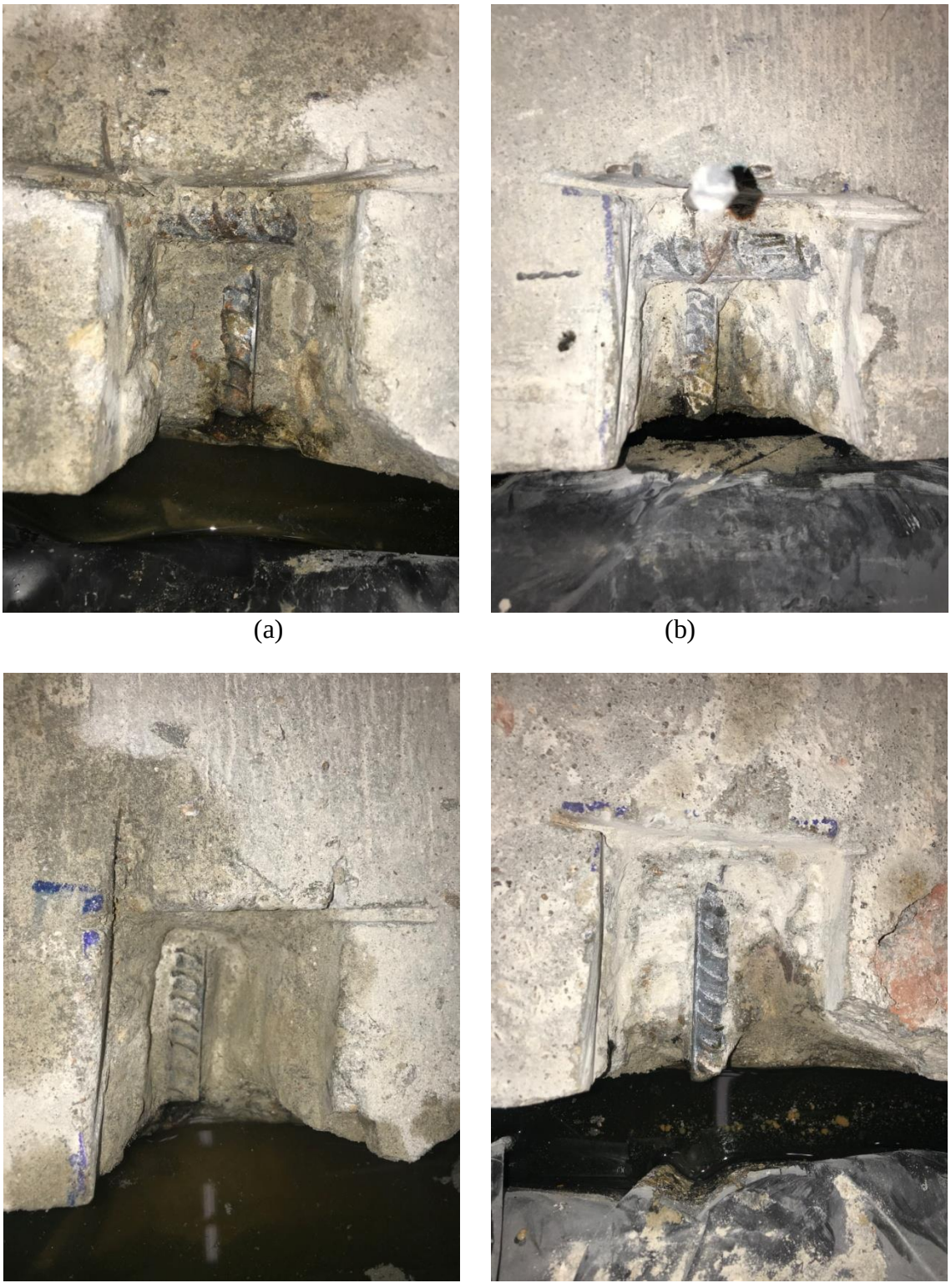

(a) (b)

(c) (d)

Figure 58: First Chip of Large-Scale Corrosion Specimens Using (a) ODOT AA (b) J3 (c) Ductal® (d) Phoscrete

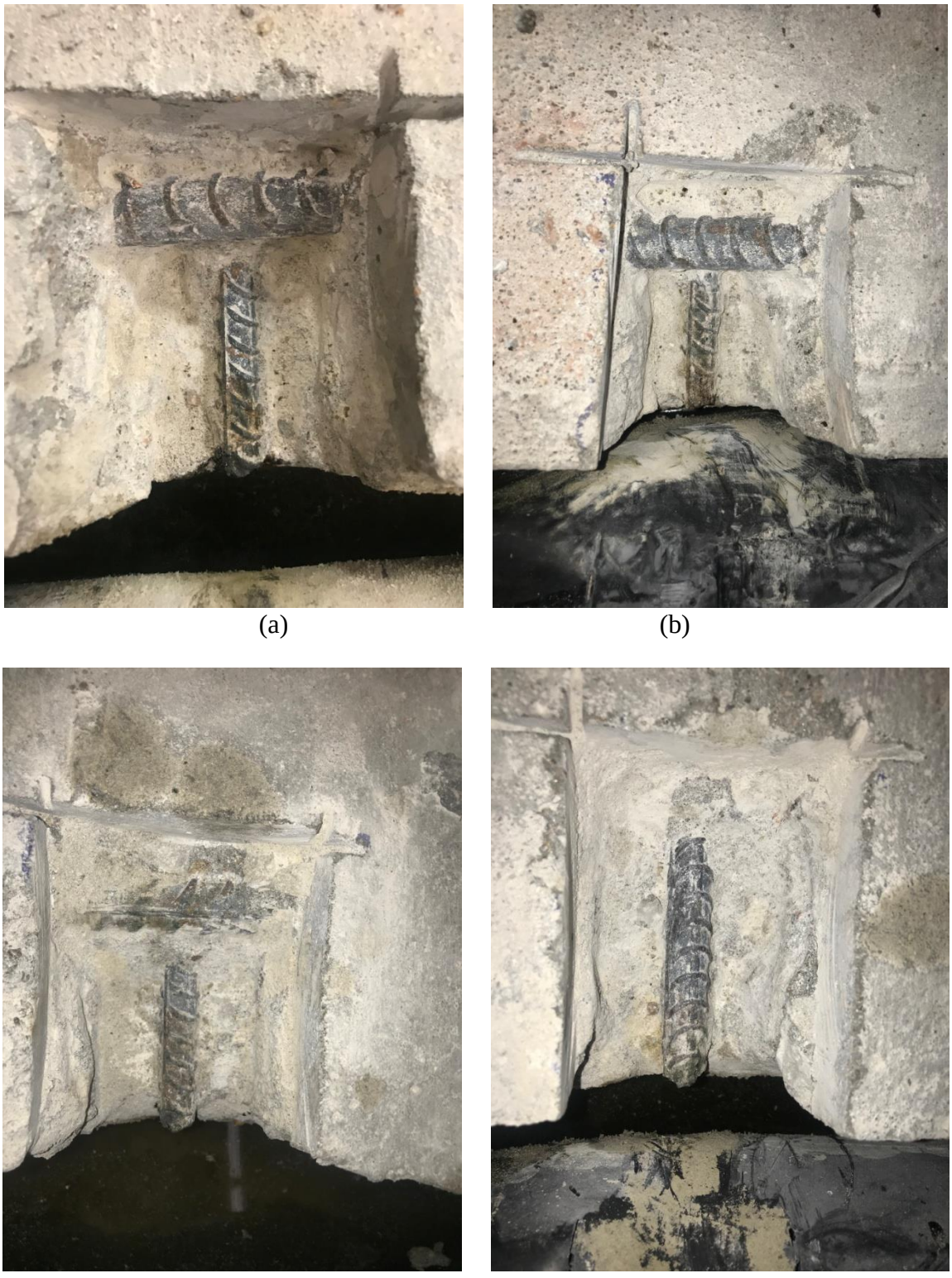

(a) (b)

(c) (d)

Figure 59: Second Chip of Large-Scale Corrosion Specimens Using (a) ODOT AA (b) J3 (c) Ductal® (d) Phoscrete



(a) (b)

(c) (d)

Figure 60: Fourth Chip of Large-Scale Corrosion Specimens Using (a) ODOT AA (b) J3 (c) Ductal® (d) Phoscrete

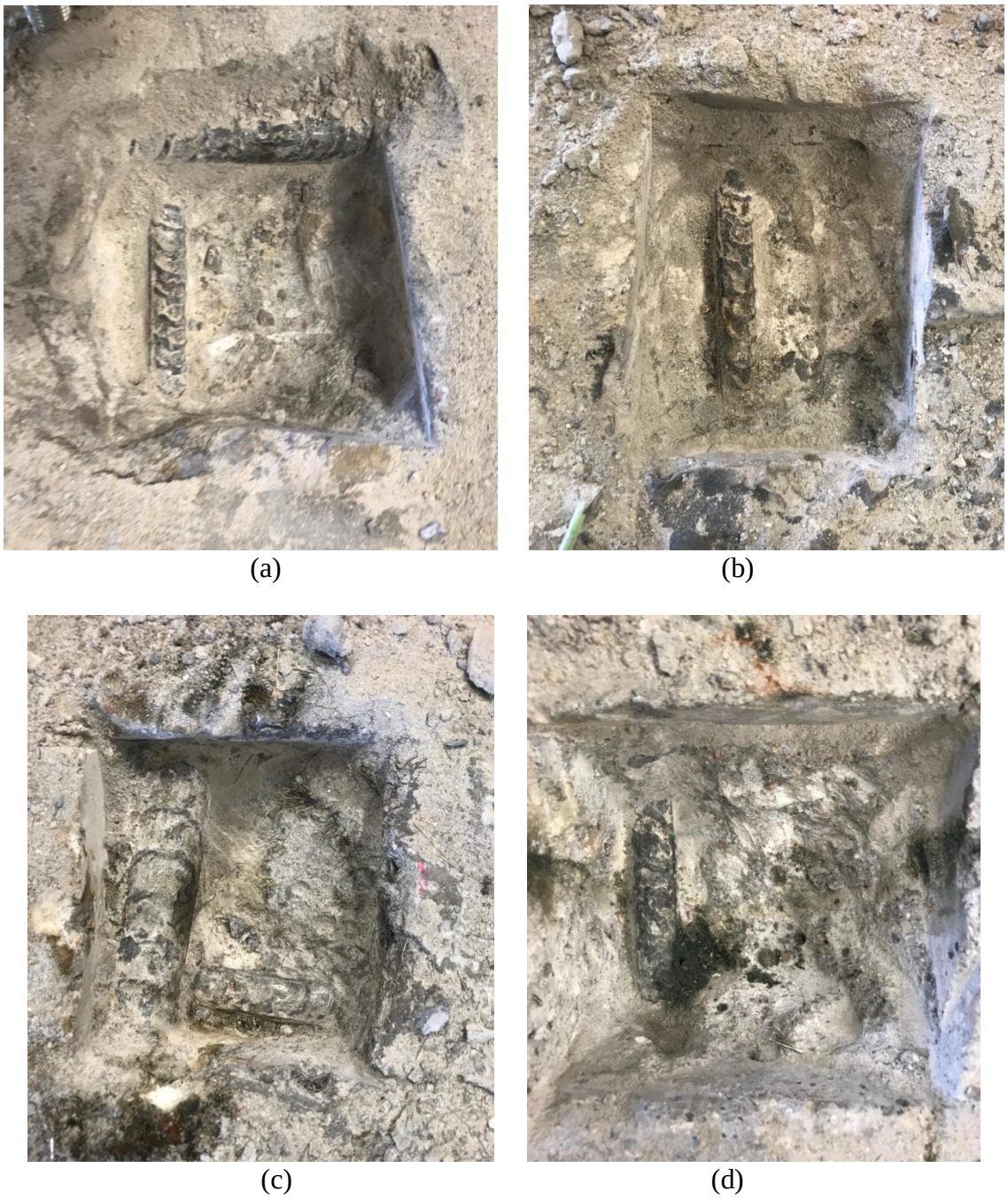

(a) (b)

(c) (d)

Figure 61: Fifth Chip of Large-Scale Corrosion Specimens Using (a) ODOT AA (b) J3 (c) Ductal® (d) Phoscrete

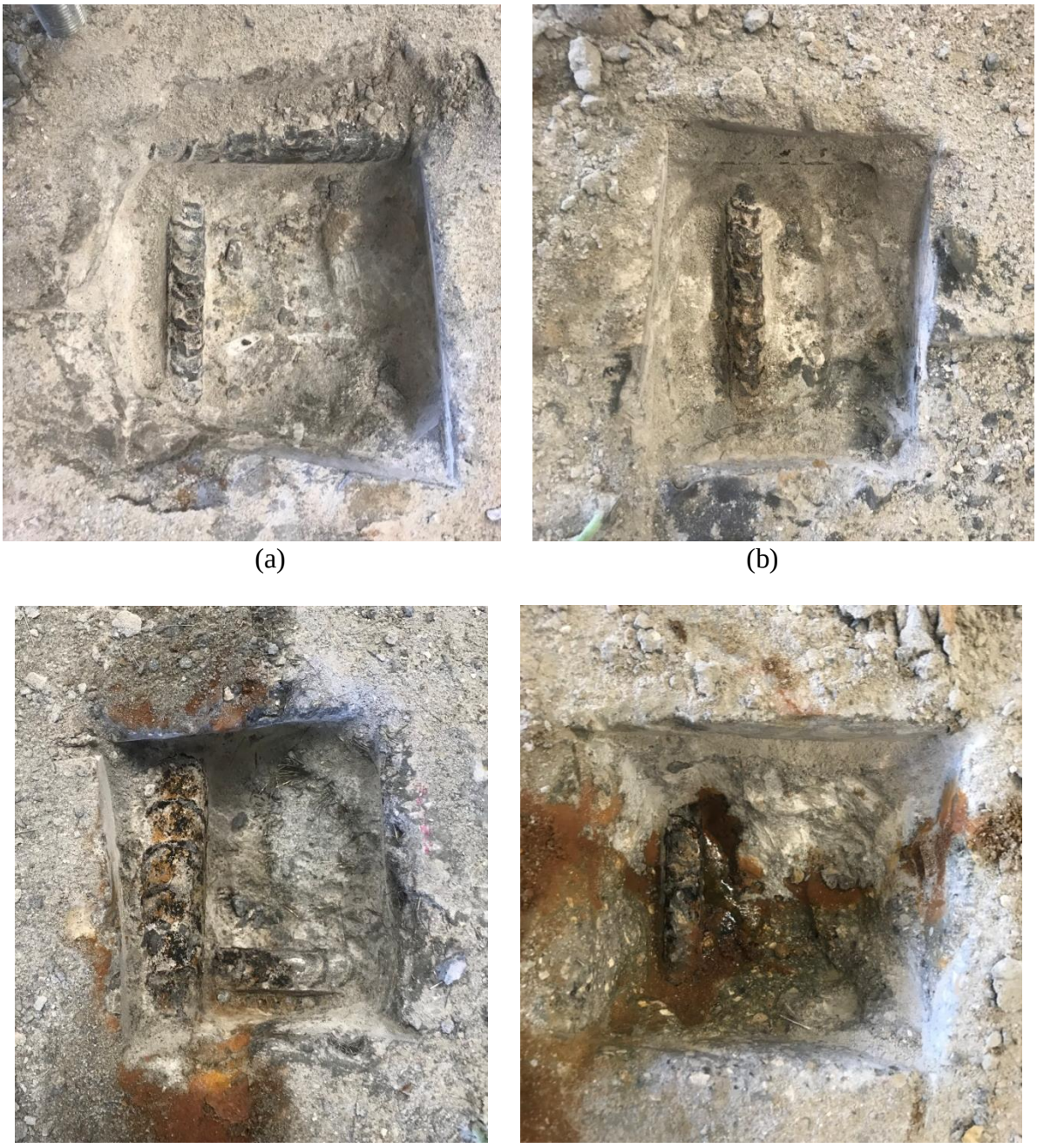

(a) (b)

(c) (d)

Figure 62: Fifth Chip of Large-Scale Corrosion Specimens 24 Hours After Chipping Using (a) ODOT AA (b) J3 (c) Ductal® (d) Phoscrete

The excavation of the reinforcing steel located in the large-scale corrosion specimens for visual examination can be broken up into two parts: excavation of rebar ends (numbers one through three) and excavation of rebar along the joint (numbers four and five). Excavations one through four were done while testing was still in progress, while excavation five was done 24 hours after testing was concluded.

Excavation one occurred after 11 days of testing and revealed slight corrosion on the reinforcing steel near the exposed end of the ODOT AA and J3 specimens (up to 0.5 in. maximum), with no corrosion visible on the reinforcing steel of the Ductal® or Phoscrete specimens. Excavation two occurred after 25 days of testing and revealed slightly more reinforcing steel corrosion than was previously seen on the ODOT AA, J3, and Phoscrete specimens, with significantly more corrosion now visible on the steel reinforcing of the Ductal® specimen (up to 1.5 inches). Though no photographs were taken of excavation three, which occurred after 40 days of testing, similar results as those seen in excavation two were achieved, with at least 1 inch of corrosion now visible on the reinforcing steel of all four specimens. This amount of corrosion was sufficient enough to indicate that reactions could be occurring along the joint of each specimen.

For that reason, excavation four was done along the same reinforcing bar revealed during excavation one, only now at the joint of each specimen, after 52 days of testing. This excavation revealed roughly 0.5 inches of surficial corrosion on the ODOT AA specimen, starting at the joint and moving into the repair material side, trace amounts of pitting corrosion around the joint of the J3 and Phoscrete specimens, and heavy amounts of pitting corrosion and staining

occurring at the joint of the Ductal® specimen, as if the corrosion was actively coming through the joint.

Excavation five was done after 70 days of testing and was done on the closest layer of rebar to the inflow of current, again along the joint of each specimen to directly monitor the "Halo Effect" occurring in these specimens. This location did overlap the area in which the various liquids were coming out of the joints of the Ductal® and Phoscrete specimens in the hope to find the effect of these liquids on the encompassed steel reinforcing.

Ultimately, there was a surprisingly small amount of corrosion revealed on the ODOT AA specimen, likely because its pH was closest to that of the old concrete, so it did not have as strong of a reaction as the other repair materials did to this type of large-scale testing set-up. The two UHPC repair materials did not hold up quite as well, with J3 showing minor surficial corrosion along the joint and Ductal® showing major pitting and surficial corrosion starting at the joint and working its way completely through both of the visible pieces of reinforcing steel on the base concrete side. Figure 63 attests to the varying levels of complete surface corrosion by presenting pieces of the concrete that were chipped away during excavation five that have pulled away surficial corrosion, i.e., Figure 63(a) shows a piece of base concrete with minor surficial corrosion on the side that made up the joint of the J3 specimen, while Figure 63(b) shows multiple pieces of base concrete that have been completely covered on multiple sides with heavy surficial corrosion, all from the Ductal® specimen.

Significantly worse, however, was the response of the Phoscrete specimen to excavation. Within 60 seconds of revealing the reinforcing, a puddle of the green liquid that had been present on the surface of the specimen since week 7 began to leak from the joint, until it reached the point shown in Figure 61(d) and seemed to steady out. After 24 hours however, the liquid had spread and corroded to the point shown in Figure 62(d). Slight pitting corrosion was also immediately visible along the reinforcing steel at the joint of the Phoscrete specimen, which was only exacerbated by the presence of the liquid leaking through. This observation proved that the green liquid seen on the surface of the Phoscrete specimen had to have been coming through the joint to the surface, and was something made and stored within the concrete, since the specimen was taken completely out of the testing set-up and exposed to air for the 24 hour waiting period, so it could not just be the surrounding NaCl solution leaking through.

Figure 63(c) shows pieces of the base concrete that were chipped away during excavation five of the Phoscrete specimen and not only shows the presence of surficial corrosion along the joint of the Phoscrete specimen (like that shown in Figures 63(a) and 63(b) for J3 and Ductal®, respectively) but also the presence of the kind of staining caused by the green liquid that has leaked through the joint, proving that the liquid was present even before excavation.



(a)



(b)



(c)

Figure 63: Evidence of Surficial Corrosion on Large-Scale Corrosion Specimens Using (a) J3 (b) Ductal® (c) Phoscrete

In addition to the visual examination data, measurements of the change in voltage measured by each of the power supplies throughout the study were taken (Figure 64). In other words, the amount of voltage required to supply each specimen with the 0.2 A of current used throughout testing was recorded on various dates during testing for comparison. This data is important because a larger voltage represents more energy being needed by the power supply to get the 0.2 A of current all the way through the specimen and back to the power supply. This in turn shows the resistance of the specimen to the flow of corrosion-inducing cycles, like the electrochemical (forced current) method used in this testing, with the specimen with the highest voltage readings being the most resistant. Based on these readings J3 showed to be the overall most resistant, with Phoscrete being the overall least resistant. These findings are very much in line with the visual examinations of both the small- and large-scale specimens.

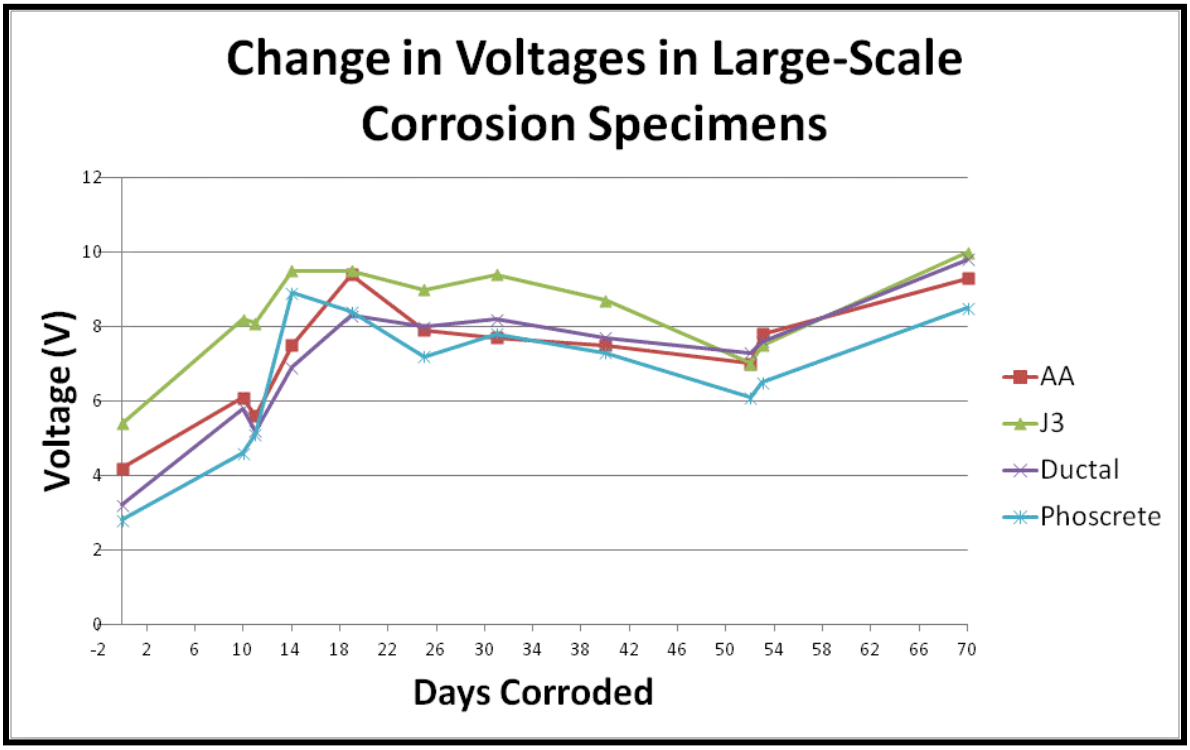

Figure 64: Graph of the Change in Voltage over Time of all Large-Scale Corrosion Specimens

As mentioned in 5.2.3, the response of Phoscrete to both small- and large-scale corrosion testing has raised much concern, and additional testing is advised to assess Phoscrete's durability and corrosion properties to fully understand its viability in the field. The final state of the south side of the large-scale Phoscrete corrosion specimen, the side that experienced the secretion of the unknown green liquid is shown in Figure 65, which reveals the entire end to be a dark green color. This overall completely unique corrosion response of the large-scale corrosion specimen is the primary cause for concern for using Phoscrete on future projects in potentially corrosive environments.



Figure 65: Final State of Phoscrete Large-Scale Corrosion Specimen- Week 10

5.3.3 Summary of Results

Similar to the small-scale corrosion testing, visual examination is the only tool available for analyzing the final results of this large-scale corrosion testing. However, also similarly to the small-scale corrosion testing, this is not a significant issue, because the goal of this testing was to verify the adequate performance of the non-proprietary UHPC mix design J3 under rapid corrosion, and this result was undoubtedly achieved. Though out-performed slightly by the standard ODOT AA mixture, J3 performed significantly better than the proprietary products Ductal® and Phoscrete throughout large-scale testing, both through overall corrosion levels, and the distinct lack of any type of surface joint corrosion or leakage.

This result, coupled with the extremely superior performance of J3 during small-scale corrosion testing (out-performing the ODOT AA mix and achieving similar results to that of Ductal®) and the known strength and durability advantages J3 has over ODOT Class AA concrete (as discussed in Chapter 1 and Chapter 4, respectively) proves J3 to be suitable for trial use in the field.

6.0 Findings, Conclusions, and Recommendations

The following chapter summarizes the findings, conclusions, and recommendations from this research study.

6.1 Findings

6.1.1 Durability Testing

The following findings were observed during durability testing:

- The first round of chloride ion penetration testing was performed with UHPC specimens containing steel fibers and produced results that did not reflect the actual response of the UHPC specimens.
- During both 28 and 90 day chloride ion penetration testing, the ODOT AA specimens had moderate visual corrosion spotting, with both the Ductal® and J3 specimens having no visual corrosion spotting.
- Chloride ion penetration testing results of the ODOT AA mix were all in the low to moderate range.
- Chloride ion penetration testing results of both Ductal® and J3 were all in the negligible to very low range.
- All chloride ion penetration values reduced between 28 and 90 days of testing due to continued hydration of the specimens between testing periods.

- ODOT AA freeze-thaw cycling specimens all showed significant surface deterioration after 350 cycles, although the internal structural integrity remained high, ultimately resulting in a final average RDM of 99%.
- Both Ductal® and J3 had final average RDM values of approximately 103% and exhibited only slight surface deterioration by the end of freeze-thaw cycling.
- Scaling resistance testing of ODOT AA specimens resulted in a normal amount of surface deterioration for traditional concrete, with an average final visual rating of 1.75.
- Ductal® specimens responded unexpectedly poorly to scaling resistance testing, experiencing similar levels of surface deterioration to that of the ODOT AA specimens, with an average final visual rating of 1.25.
- J3 specimens responded exceptionally well to scaling resistance testing, experiencing no surface deterioration throughout testing, resulting in an average final visual rating of 0.
- In both the freeze-thaw cycling and scaling resistance testing, Ductal® had significant surface corrosion of steel fibers, whereas J3 specimens only experienced extremely mild surface corrosion of steel fibers, even though the J3 specimens used the same steel reinforcing fibers in similar quantities.

6.1.2 Corrosion Testing

The following findings were observed during corrosion testing:

- The Halo Effect was not strong enough in any of the small-scale specimens to result in enough corrosion to create a measurable macrocell current across the two different

concrete halves during the allotted 10 week testing period. A small macrocell current was measured across adjacent reinforcing bars.

- ODOT AA experienced mild corrosion of steel reinforcing at the joint due to the Halo Effect during small-scale corrosion testing but very little steel reinforcing corrosion due to the Halo Effect during large-scale corrosion testing.
- Ductal® experienced very little corrosion of steel reinforcing at the joint due to the Halo Effect during small-scale corrosion testing but significant steel reinforcing corrosion due to the Halo Effect during large-scale corrosion testing.
- J3 experienced very little corrosion of steel reinforcing at the joint due to the Halo Effect during both small- and large-scale corrosion testing.
- Phoscrete experienced significant corrosion of steel reinforcing at the joint due to the Halo Effect during both small- and large-scale corrosion testing.
- Ductal® displayed significant visible surface corrosion along the joints of all small- and large-scale corrosion specimens. This corrosion was due to the Halo Effect, not an issue with bonding, since Ductal® was proven in previous Phase I testing to have excellent bonding to all surface types and this response was consistent across all specimens, even across different testing set-ups (small- and large-scale testing).
- Phoscrete exhibited a strong negative reaction to corrosion testing. This included the production of a white film in the 5% NaCl solution used in both small- and large-scale testing, as well as the production of a dark green liquid along the surface of the joint at the south-end of the large-scale specimen. By the end of testing, the entire south-end of the large-scale specimen was covered in dark green corrosion product along the bottom and side surfaces.

6.2 Conclusions

Based on the previously outlined findings, the following conclusions were developed:

- The use of normally-saturated (air dried) fine masonry sand instead of oven-dried did not affect the strength or durability properties of J3.
- For all future chloride ion penetration testing, UHPC specimens should be cast without steel fibers to achieve accurate test results.
- J3 matched Ductal® in all durability testing and even surpassed Ductal® in corrosion resistance, despite not having any silica powder or microsilica, which is utilized in Ductal® as the finest level of particles achievable for additional particle packing. This is probably because the GGBFS used in the J3 mix design is sufficiently small enough to make up for this lack of silica powder or microsilica.
- ODOT Class AA concrete is sufficient for use in the field in moderate-corrosive environments, and causes very little corrosion in steel reinforcing due to the Halo Effect during repairs.
- Ductal® is the standard for durability properties for UHPC, although it experiences high levels of corrosion along the joint of repairs due to the Halo Effect, which is a potential cause for concern.
- J3 is sufficient for use in the field based on both durability properties and corrosion resistance.
- J3 is sufficient for use in projects where UHPC's additional durability is desirable, such as highly corrosive environments or area's prone to freezing and thawing.

- Phoscrete should not be used as a repair material in highly corrosive areas until its corrosion response is better understood and proven to be within acceptable bounds.

6.3 Recommendations

The goal of this study was to investigate the durability and corrosion response of the non-proprietary UHPC mix design J3 to determine how reliable and effective it will be in the field. The findings and conclusions drawn from this thesis research led to the following recommendations for future study:

- Install and monitor J3 in a field application.
- Perform durability testing of Phoscrete, including: freeze-thaw, scaling, and chloride ion testing.
- Complete further corrosion testing of Phoscrete to determine if the response observed in large-scale corrosion testing would occur under field conditions.
- Determine whether Ductal® is currently experiencing corrosion along the joint of repairs in the field, how detrimental this is to the strength of the reinforcing steel, and if there is any way to prevent/slow this response.
- Complete further durability and corrosion testing of similar non-proprietary UHPC mix designs to continue to examine the viability of using non-proprietary mixes such as J3.

7.0 Appendices

7.1 Tables

Table 22: Measured Voltage (V) at Conclusion of Initial Testing Between Adjacent Steel Reinforcing Bars in 0% NaCl Small-Scale Corrosion Specimens

Concrete Type	1 to 2	1 to 3	2 to 3	4 to 5	4 to 6	5 to 6
AA	-68.8	-7.2	61.4	-68.6	-7.0	61.8
J3	9.9	159.9	149.8	10.3	159.9	149.5
Ductal®	-84.6	-64.6	-20.4	-83.9	-63.8	-20.1
Phoscrete	11.9	11.5	-0.4	11.9	11.5	-0.4

Table 23: Graybeal (2018) Study Mix Design in lb/yd^3

Name	Cement	Silica Sand	Ground Quartz	Silica Fume	Liquid Admixtures	Water	Fibers
U-A	1,328	1,288	367	518	23	278	416
	Pre-Blended, Pre-Bagged Powder				Liquid Admixtures	Water	Fibers
U-B	3,516				48	354	267
U-C	3,000				0	268	612
U-D	3,700				89	219	263
U-E	3,236				73	379	263

Table 24: Graybeal (2018) Study Durability Results

Name	Average Coulombs Passed at 28 Days	Average Coulombs Passed at 56 Days	RDM After 600 Cycles (%)
U-A	302	53	102.5
U-B	5100	2501	103
U-C	425	298	99
U-D	789	495	101
U-E	470	303	100

7.2 Figures

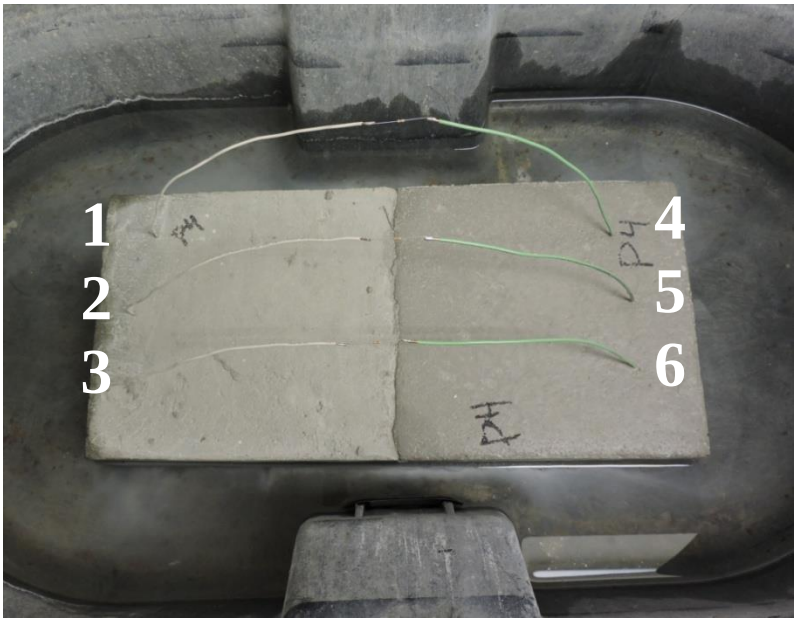

Figure 66: Numbering for Measurements of Voltage Between Adjacent Steel Reinforcing Bars

8.0 References

AASHTO T 277e86, Rapid Determination of the Chloride Permeability of Concrete, American Association of States Highway and Transportation Officials, Standard Specifications - Part II Tests, Washington, D. C., 1990.

Abosrra, L., Ashour, A. F., and Youseffi, M. (2011) "Corrosion of steel reinforcement in concrete of different compressive strengths," *Construction and Building Materials*, 25(10): 3915-3925.

Ahlborn, Theresa M. "Characterization of Strength and Durability of Ultra-High- Performance Concrete under Variable Curing Conditions." *ILLiad Logon*, 2011, ll.libraries.ou.edu/illiad.dll?Action=10&Form=75&Value=105041. pp. 68-75.

Alkaysi, Mo, et al. "Effects of Silica Powder and Cement Type on Durability of Ultra-High Performance Concrete (UHPC)." *ScienceDirect*, 2016.

ASTM Standard C666 (2015) "Standard Test Method for Resistance of Concrete to Rapid Freezing and Thawing," ASTM International, West Conshohocken, PA.

ASTM Standard C672 (2012) "Scaling Resistance of Concrete Surfaces Exposed to Deicing Chemicals," ASTM International, West Conshohocken, PA.

ASTM Standard C1202 (2017) "Standard Test Method for Electrical Indication of Concrete's Ability to Resist Chloride Ion Penetration," ASTM International, West Conshohocken, PA.

Cervo, Nicholas M., and Andrea J. Schokker. "Bridge Deck Patching Material Evaluation." *Journal of Bridge Engineering*, vol. 15, no. 6, 2010, pp. 723-730., doi:10.1061/(asce)be.1943-55920000109.

Chumping, GU, et al. "Effect of Curing Conditions on the Durability Pf Ultra-High Performance Concrete under Flexural Load." *OU Library*, 2015, link-springer-com.ezproxy.lib.ou.edu/content/pdf/10.1007%2Fs11595-016-1365-0.pdf.

"What Is Macrocell Corrosion? - Definition from Corrosionpedia." *Corrosionpedia*, 2018, ww.corrosionpedia.com/definition/6336/macrocell-corrosion.

Floyd, R.W., and Volz, J. S., "ODOT Research Project Proposal: Evaluation of Ultra-High Performance Concrete for Use in Bridge Connections and Repair" The Board of Regents of the University of Oklahoma, Jul 2016.

Floyd, R.W., and Volz, J. S., "Evaluation of Ultra-High Performance Concrete for Use in Bridge Connections and Repair: Phase II Partial Depth Replacements, Bond, and Corrosion Behavior" The Board of Regents of the University of Oklahoma, May 2018.

Graybeal, Benjamin, and Jussara Tanesi. “Durability of Ultra-High Performance Concrete.” *Journal of Materials in Civil Engineering*, 2007.

Graybeal, Benjamin, “Material Property Characterization of Ultra-High Performance Concrete” FHWA-HRT-06-103, Aug. 2006, pp. 1-188.

Graybeal, Benjamin. “Properties and Behavior of UHPC-Class Materials .” FHWA-HRT-18-036, Mar. 2018, pp. 1–170.

Graybeal, B., “Tech Note | Ultra-High Performance Concrete,” FHWA-HRT-11-038, March 2011, Federal Highway Administration, McLean, VA.

Hansson, C.M., et al. “Macrocell and Microcell Corrosion of Steel in Ordinary Portland Cement and High Performance Concretes.” ac.els-cdn.com/S000888460600192X/1-s2.0-S000888460600192X-main.pdf?_tid=b0e5e44c-b229-4791-b82b-1e5c880e0153&acdnat=1541811819_2a3926ed8add167725674d70f7ad472a., *ScienceDirect,* 2006

Jones, Denny A. *Principles and Prevention of Corrosion*. Prentice-Hall, 1996.

McDaniel, Amy. “Development of Non-Proprietary Ultra-High-Performance Concrete Mix Designs.” *University of Oklahoma*, 2017, pp. 1–100.

Mcdonagh, Michael, and Andrew Foden. “Benefits of Ultra-High Performance Concrete for the Rehabilitation of the Pulaski Skyway.” *Proceedings of the First International Interactive Symposium on UHPC*, 2016, doi:10.21838/uhpc.2016.91.

Mcdonagh, Michael, and Andrew Foden. “Benefits of Ultra-High Performance Concrete for the Rehabilitation of the Pulaski Skyway.” *Proceedings of the First International Interactive Symposium on UHPC*, 2016, doi:10.21838/uhpc.2016.91.

Sprinkel, Michael, director. *Corrosion of Reinforcement in UHPC. YouTube*, American Concrete Institute, 27 Jan. 2015, www.youtube.com/watch?v=nXFD4HnICmU.

Resplendino, Jacques, and Toutlemonde François. *Designing and Building with UHPFRC: State of the Art and Development*, ISTE, 2011, pp. 199, 377-386, 706.

Wang, L., Yi, J., Zhang, J., Jiang, Y., Zhang, X. (2017) “Effect of corrosion-induced crack on the bond between strand and concrete,” *Construction and Building Materials*, 153: 598-606.